3-2006

Active Optical Tracking with Spatial Light Modulators

Steven R. Mawhorter

Active Optical Tracking with Spatial Light Modulators

THESIS

Steven R. Mawhorter, Second Lieutenant, USAF

AFIT/GE/ENG/06-40

DEPARTMENT OF THE AIR FORCE
AIR UNIVERSITY

AIR FORCE INSTITUTE OF TECHNOLOGY

Wright-Patterson Air Force Base, Ohio

AFIT/GE/ENG/06-40

Active Optical Tracking with Spatial Light Modulators

THESIS

Presented to the Faculty

Department of Electrical and Computer Engineering

Graduate School of Engineering and Management

Air Force Institute of Technology

Air University

Air Education and Training Command

In Partial Fulfillment of the Requirements for the

Degree of Master of Science in Electrical Engineering

Steven R. Mawhorter, B.S.E.E.

Second Lieutenant, USAF

March 2006

AFIT/GE/ENG/06-40

Active Optical Tracking with Spatial Light Modulators

Steven R. Mawhorter, B.S.E.E.
Second Lieutenant, USAF

Approved:

/signed/	06 Mar 2006
Lt Col Matthew Goda, PhD Thesis Advisor	date
/signed/	06 Mar 2006
Dr. Steven Cain Committee Member	date
/signed/	06 Mar 2006
Dr. Michael Marciniak Committee Member	date

Abstract

Two spatial light modulators (SLMs) are utilized for beam splitting, steering and tracking. Both linear and holographic phase screens are used in a demonstration of technology to allow real time tracking to communicate in a one-to-several type scenario. One SLM is used to apply a linear phase modulation to steer multiple beams onto a detector. The spots that are produced represent the targets as they move around the field of view of the central communication node. A Gerchberg-Saxton algorithm will subsequently use the detected spots as the desired pointing locations. Using this as input, the Gerchberg-Saxton algorithm yields a phase only map for multiple spot beam steering which is called the holographic phase. The holographic phase screens are then used on a second SLM to steer beams onto the same detector in near real time. As the target spots move about the detector's field of view, the holographic spots track them.

Acknowledgements

First and foremost, I need to express how much I appreciate my wife Sydney for the support she gave me on this thesis. Also, for allowing me to be mostly absent from family affairs for the months it took to complete this project. I am grateful for the moral support and assistance with MATLAB® & LaTeX® that Neil and Jody Paris provided. I would like to thank Lt Col Goda and the rest of the thesis committee for their time and feedback given on this thesis. I owe a large debt of gratitude to Jason Schmidt whose almost daily instruction and guidance vastly improved the quality of the results achieved.

Steven R. Mawhorter

Table of Contents

List of Figures

List of Abbreviations

Active Optical Tracking with Spatial Light Modulators

I. Introduction

1.1 Motivation

The Air Force currently has a need for optical beam steering in many different applications. There are several ways to accomplish the task of beam steering. Historically, the most common method employed to steer a beam is the use of a simple mirror. When a mirror is used in conjunction with a controller to move the mirror, precise and dynamic steering can take place. These control systems usually involve the extensive use of mechanical systems, often with a gimbal. However, these mechanical systems have moving parts with inertial resistance which can limit the steering speed of the system. Beam steering to multiple locations with a gimballed mirror is not possible. Also, the size, weight, and power consumption of such gimballed steering systems just are not sufficient for many current Air Force applications.

1.2 Problem Statement

The research presented in this thesis focuses on the development of procedures to manipulate non-linear holographic techniques combined with spatial light modulators (SLM) for the purposes of tracking and steering light to multiple targets in a communications scenario.

1.3 Research Objectives

- Develop phase screens to steer a beam to a single location using linear and holographic methods in simulation.
- Use a phase only device (SLM) to apply the developed phase screens in a laboratory environment to steer a beam.

- Dynamically split and steer a beam to multiple locations using linear and holographic phase screens in simulation and with a SLM.
- Compare effects of using linear and holographic phase screens on spot quality.
- Demonstrate near real time tracking of multiple targets using the holographic techniques developed.

1.4 Overview

Chapter 2 presents a thorough discussion of beam steering and the conditions necessary for it to take place. The law of reflection and blazed gratings will be covered first, to be followed by a section on Fourier analysis. The Fourier analysis will provide the mathematics needed to show that a linear phase delay will steer an optical field. Another steering method using the Gerchberg-Saxton algorithm called the Holographic method will be provided. Different devices with which a beam can be steered, such as a gimballed mirror and a SLM, are covered [6]. The SLMs that are discussed consist of a technology using micro electro-optical system (MEMS), and another using liquid crystals (LC). Each steering device mentioned will be compared to the others to illustrate its advantages and disadvantages.

Chapter 3 will begin with a scenario in which a one-to-many communications link is used and discusses possible ways of realizing such a link with actual hardware and beam steering techniques. In order to explore the theory behind beam steering, and subsequently multiple beam steering, means for computer simulations are developed with the use of MATLAB®. Multiple beam steering actually involves splitting one beam and steering it to multiple locations, but the process will be referred to as multiple beam steering for brevity. Three different methods of producing phase screens capable of beam steering will be discussed. The physical setups for demonstrating beam steering with LC SLMs will be given. The optical elements used in the physical setup need to be calibrated so the process of accomplishing this will be covered. The steering methods will be compared for their resulting spot size and shaping

abilities which will effect the SNR achieved for the communication link. Dynamic beam steering will then be discussed, a process that allows beams to be steered onto moving targets. Finally, a setup will be developed with a dual SLM system for testing near-real time beam tracking on an optical bench.

Chapter 4 will begin by showing the results of the computer simulations discussed in Chapter 3. The simulations will confirm the theory given in Chapter 2. The results of the linear and holographic steering using an SLM will be presented. There will be a discussion about the shortcomings of the Holographic method. A solution to address the problems with the Holographic method is subsequently developed to yield acceptable results for beam steering. Finally, the results of an attempt at near real time beam tracking will be presented.

Chapter 5 discusses the conclusions reached during experimentation and remaining work to be accomplished. The research shows an ability to use SLMs for multiple beam steering and near real time tracking. However, this thesis does not develop an end user product. There are still issues to deal with other than the ideas and methods presented herein. Several shortcomings of the developed methods will be presented and possible solutions offered to provide solutions to them. Some new ideas will offer possible direction for further research in beam tracking and steering with SLMs.

II. Background

Beams can be steered for laser light shows, communication purposes, remote observation, target designation, to destroy targets, and for many other applications. Much of the theory needed to understand the conditions for beam steering has been known for quite some time and is presented in Section 2.1. More specifically, the Law of Reflection and blazed gratings will be covered in subsections 2.1.1 and 2.1.2, respectively. In subsection 2.1.3, Fourier analysis will give a mathematical basis to understand how a linear phase delay causes a beam to be steered. A nonlinear technique for beam steering using the Gerchberg-Saxton phase retrieval algorithm will be offered in subsection 2.1.4. Also, some of the devices that have steering capabilities will be presented. The devices discussed include a simple mirror, section 2.2, and spatial light modulators in section 2.3. Two different types of spatial light modulators will be covered. One type of SLM, in subsection 2.3.1, uses liquid crystal technology and the other, in subsection 2.3.2, uses micro-scale mirrors to apply a linear phase delay, modulo 2π, to an optical field. Finally, in Section 2.4, a comparison between the use of a gimballed mirror and the two SLM technologies is presented to highlight each device's strengths and weaknesses with respect to the other devices for beam steering purposes.

2.1 Beam Steering

Beam steering takes place with simple wavefront manipulation of an optical field. This section covers several ways in which beam steering can be understood. Historically, the Law of Reflection has been used as the model to explain how beam steering takes place and the location in which one can expect a beam to be steered. Fermat developed a more complete theory of the conditions that cause a beam to be steered. Blazed gratings have been shown to have beam steering capabilities and will be examined. Fourier analysis will show that a linear phase delay does indeed produce a spatially shifted beam spot and how the size of such a spot can be determined.

Finally, an algorithm for a relatively new way of beam steering with holographic phase screens will be presented.

2.1.1 Law of Reflection. All of us have steered light in some way. Adjusting the rear view mirror in your car at night to reduce the amount of light shining into your eyes is one simple example. Basic beam steering is governed by the first part of the Law of Reflection which states that "the angle-of-incidence, equals the angle-of-reflection" [8, page 99] This means that the angle in which light hits a reflective surface, θ_i, will bounce off at the same angle, θ_r, with respect to the normal of the surface. However, this falls short of fully describing the process of beam steering.

The conditions for beam steering to take place involve linearly changing the optical path length (OPL) of a wavefront. Fermat's principal tells us that "a light ray in going from point S to point P must transverse an optical path length that is stationary with respect to variations of that path" [8, page 109], The optical path length is the physical length, l, times the index of refraction, n.

$$OPL = nl \tag{2.1}$$

One can see there are two different ways to linearly alter the OPL and hence steer the wavefront. The first method is to linearly change l, the physical distance that an field propagates. The second method is to linearly change the index of refraction, n, that a wavefront encounters upon refracting off of a surface. Figure 2.1 gives a simple one-dimensional illustration of what a linear delay of the OPL does to a beam. If θ is the phase angle, the resulting steer angle is also θ. To cause a spatial shift, a phase delay needs to be linear but not strictly continuous.

2.1.2 Blazed Grating. A delay in OPL can be represented modulo 2π and beam steering will still take place as with the continuous delay. This technique is often employed using a blazed grating. In Figure 2.2, one can see how a modulo 2π phase imitates a continuous linear phase delay. If the blazed grating is perfect,

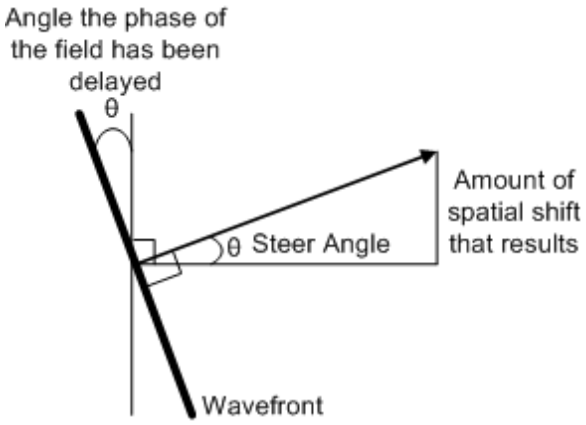

Figure 2.1: Result of linear phase delay on an optical field.

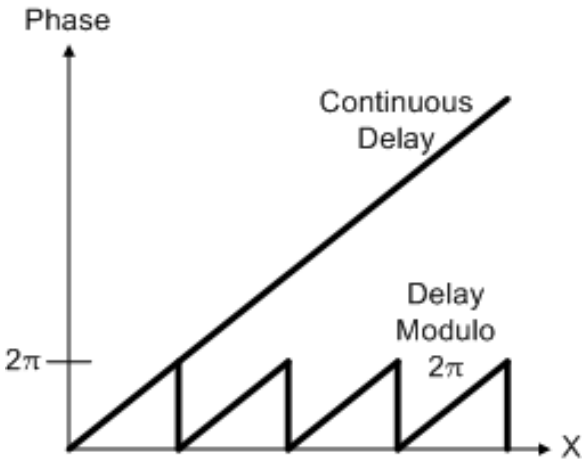

Figure 2.2: Phase grates are used to imitate a continuous phase delay modulo 2π.

then all of the power will be steered to the same location that a continuous delay would steer it to. A perfect blazed grating would have teeth that are all precisely the same width and height. However, a perfect grating cannot be manufactured, so other higher orders of diffraction are observed due to periodicity, and shown in Figure 2.3. This has the effect of lowering the diffraction efficiency to a certain order of the blazed grating pattern and shifts energy into the higher orders.

The $m = 0$ order is the location where ordinary reflection off of the surface would steer a beam to had there not been any blaze. The $m = 1$ or first order is the angle that will be of focus in this research. There are, of course, more orders than

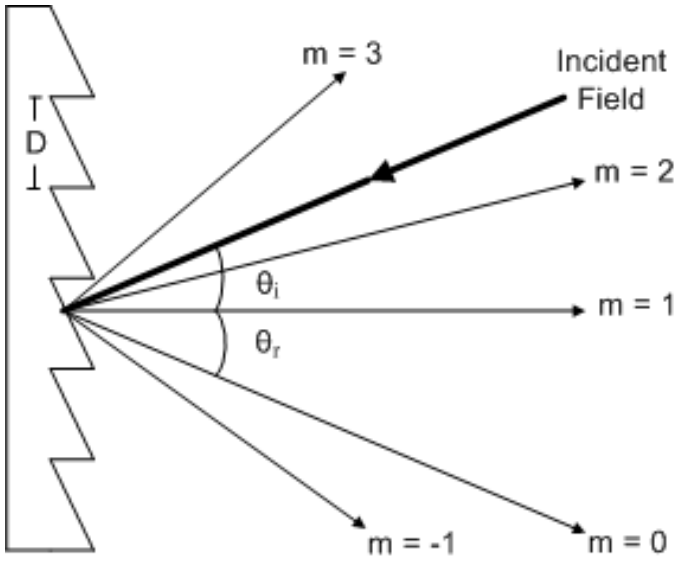

Figure 2.3: Blazed grating with some of the diffractive orders shown.

are shown in Figure 2.3. The first order is most often used for beam steering because the grating can be designed so that it is the order where most of the power will be contained, and can be steered due to the blaze angle. The grating equation, Equation 2.2, is used to find the angles at which the wavefront will be steered for a given blaze angle. The angles can be varied if the distance, D, of the grates is changed.

$$\boldsymbol{\theta}_m = \pm \arcsin\left(\frac{m\lambda}{D}\right) \tag{2.2}$$

A blazed grating can be a physical structure of mirrors or it can be produced by a change in index of refraction. The phase grates symbolize a linear change of OPL modulo 2π. A modulo 2π phase representation is commonly referred to as a type of phase screen.

2.1.3 Fourier Analysis. A linear phase delay of a beam's OPL is the cause of beam steering, but to this point, no mathematics have been used to actually prove that as a beam propagates it can be steered. An optical field that consists of a plane

wave is a solution to the wave equation. A Fourier optics approach can be used to see what happens as such a field propagates from one location to another.

The pupil plane and Fourier plane are a Fourier Transform (FT) pair shown in Figure 2.4. This means that if a field encounters a linear phase delay in the pupil plane, a spatial shift will occur in Fourier plane. For a collimated beam, the Fourier plane and the image plane coincide with each other. This means that a linear phase shift that occurs in the pupil plane will result in a spatial shift in the image plane. The equations used throughout this subsection are developed from first principles in [3]. Next, the mathematics behind the propagation and steering of a field are presented.

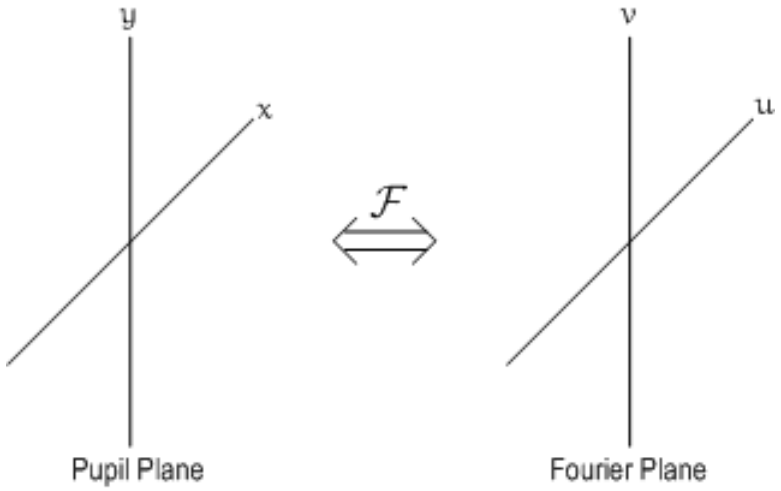

Figure 2.4: The pupil and Fourier planes are Fourier Transform pairs.

Analysis of optical field propagation often begins with the Fresnel-Kirchoff diffraction integral, where $U(u, v, z)$ is the field in the image plane, $U(x, y, 0)$ is the field in the pupil plane, z is the distance between the two planes, and k is the wave number.

$$U(u,v,z) = \frac{\mathrm{e}^{\mathrm{i}kz}}{\mathrm{i}\lambda z} \int_{-\infty}^{\infty}\int_{-\infty}^{\infty} U(x,y,0)\ \mathrm{e}^{\frac{\mathrm{i}k}{2z}[(u-x)^2+(v-y)^2]}\ \mathrm{d}x\ \mathrm{d}y \tag{2.3}$$

If the quadratic term in the integral is multiplied out, the $\mathrm{e}^{\frac{ik}{2z}(u^2+v^2)}$ term factored out of the integral, the substitutions $u = \lambda z f_x$ and $v = \lambda z f_y$ made in the exponential with the cross terms, then Equation 2.4 is obtained where $\mathcal{F}$ denotes the FT.

$$U(u,v,z) = \frac{\mathrm{e}^{\mathrm{i}kz}}{\mathrm{i}\lambda z}\ \mathrm{e}^{\frac{\mathrm{i}k}{2z}(u^2+v^2)}\ \mathcal{F}\{U(x,y,0)\ \mathrm{e}^{\frac{\mathrm{i}k}{2z}(x^2+y^2)}\}_{f_x=\frac{u}{\lambda z},f_y=\frac{v}{\lambda z}} \tag{2.4}$$

If $U(x,y,0)$ represents the field just before a circular lens, which has phase transformation,

$$t_l(x,y) = \mathrm{e}^{-\frac{\mathrm{i}k}{2f}(x^2+y^2)} \tag{2.5}$$

then the quadratic terms cancel and propagation of a field can be found using

$$U(u,v,z) = \frac{\mathrm{e}^{\mathrm{i}kz}}{\mathrm{i}\lambda z}\ \mathrm{e}^{\frac{\mathrm{i}k}{2z}(u^2+v^2)}\ \mathcal{F}\{U(x,y,0)\}_{f_x=\frac{u}{\lambda z},f_y=\frac{v}{\lambda z}} \tag{2.6}$$

A detector only sees irradiance, so the phase factors in front of the FT are eliminated and a simple FT relationship between pupil plane and image plane results.

Fourier techniques provide the basic mathematics needed to understand what happens to an optical field as it propagates after experiencing a linear phase delay. For example, if a collimated uniform field with unit amplitude, $U(x,y;0)$, is delayed by a linear phase, $e^{-j2\pi(ax+by)}$, then by using Equation 2.6, it can be shown that a shift in the image plane will result.

$$\begin{aligned}
U(u,v;z) =&\ \mathcal{F}\{U(x,y;0)e^{-j2\pi(ax+by)}\}_{f_x=\frac{u}{\lambda z},f_y=\frac{v}{\lambda z}} \\
=&\ \left\{\int_{-\infty}^{\infty}\int_{-\infty}^{\infty} U(x,y;0)e^{-j2\pi(ax+by)}e^{-j2\pi(xf_x+yf_y)}\mathrm{d}x\mathrm{d}y\right\}_{f_x=\frac{u}{\lambda z},f_y=\frac{v}{\lambda z}} \\
=&\ \left\{\int_{-\infty}^{\infty}\int_{-\infty}^{\infty} U(x,y;0)e^{-j2\pi[x(f_x+a)+y(f_y+b)]}\mathrm{d}x\mathrm{d}y\right\}_{f_x=\frac{u}{\lambda z},f_y=\frac{v}{\lambda z}} \\
=&\ \left\{\int_{-\infty}^{\infty}\int_{-\infty}^{\infty} U(x,y;0)e^{-j2\pi[x(\frac{u}{\lambda z}+a)+y(\frac{v}{\lambda z}+b)]}\mathrm{d}x\mathrm{d}y\right\}_{f_x=\frac{u}{\lambda z},f_y=\frac{v}{\lambda z}}
\end{aligned} \tag{2.7}$$

Now, make the substitution of $u' = \frac{u}{\lambda z} + a$ and $v' = \frac{v}{\lambda z} + b$ to get

$$\begin{aligned} U(u,v;z) = & \left\{ \int_{-\infty}^{\infty} \int_{-\infty}^{\infty} U(x,y;0) e^{-j2\pi[xu'+yv']} \mathrm{d}x\mathrm{d}y \right\}_{f_x=\frac{u}{\lambda z}, f_y=\frac{v}{\lambda z}} \\ & = \mathcal{U}(u',v';0) \\ & = \mathcal{U}(\frac{u}{\lambda z} + a, \frac{v}{\lambda z} + b; 0) \end{aligned} \tag{2.8}$$

Since U(x,y;0) is a collimated uniform field, then

$$U(x,y;z) = (\lambda z)^2 \ \delta(u + a\lambda z, v + b\lambda z; 0) \tag{2.9}$$

which is a delta function at the shifted coordinates of $u + a\lambda z$ and $v + b\lambda z$. Hence, the phase delay on the collimated uniform field, $U(x,y;0)$, produced a spatial shift of the delta function in the image plane. Also, the amount of shift depends on z. The dependence on z makes sense because the further the field propagates from the pupil plane, the more shift that should occur. Thus far, it has been assumed that the aperture and field are infinite. If the field is constrained by a circular aperture with a radial distance, ω, a Jinc pattern is produced.

A Jinc pattern, commonly known as an Airy spot, shown in Equation 2.10, is a well known result of diffraction theory.

$$I(r) = (\frac{A}{\lambda z})^2 \ [2\frac{J_1(k\omega r/z)}{k\omega r/z}]^2 \tag{2.10}$$

$I(r)$ represents the magnitude of the irradiance that results in a radial distance, r, from the optical axis. The Airy pattern that was produced in this case is due to the fact that a circular lens was used to perform the FT on $U(x,y,0)$. In general, the far field pattern of a collimated uniform field that propagates through a field limiting aperture is the FT of the shape of that aperture.

The Airy pattern that resulted from the above analysis has a large spot of light centered at the shifted coordinates which is surrounded by thin rings. The full width of the central lobe can be found, where D_{ap} is the diameter of the aperture from which the spot is produced.

$$d_{spot} = \frac{2.44\lambda z}{D_{ap}} \tag{2.11}$$

The width, or diffractive spreading, that occurs is reduced if the spot is produced with a larger aperture. Remember, a delta function results if the aperture and field is of infinite extent, so the larger the field emerging from an aperture, the closer one comes to achieving a delta function. Smaller spots of light will increase the signal to noise ratio (SNR). Therefore, when steering a beam, one usually wants to achieve the tightest or smallest spot possible. The best achievable spot size will be an issue when beam steering with different methods is discussed in Chapters 3 and 4.

With the use of a digital computer to solve the FT of an optical field, the discrete version of the Fourier transform (DFT) is needed. When a DFT is implemented, a certain frequency spacing results due to the sampling that took place in the original domain. The spacing that results in the frequency domain is $\mathrm{d}f = \frac{1}{N\mathrm{d}x}$. When the substitution $f = \frac{u}{\lambda z}$ was made in deriving Equation 2.6, a substitution for the differential $\mathrm{d}f = \frac{\mathrm{d}u}{\lambda z}$ was also needed. The resulting image plane spacing is shown in Equation 2.12. This image plane spacing will turn out to be important when the results from the actual experiments are examined in Chapter 4.

$$\mathrm{d}u = \frac{\lambda z}{N\mathrm{d}x} \tag{2.12}$$

The phase term, $e^{\frac{ik}{2z}(x^2+y^2)}$, in Equation 2.4 goes to zero as z gets large. When this phase term is approximately zero, the field is said to have reached the far field. As already mentioned, the phase from a lens cancels this phase term and the brings the far field pattern to the image plane of the lens. The image pattern in the far field is the Fourier transform of the field in the pupil plane. Now that the far field pattern is occurring in the image plane of the lens, it is often thought that a lens performs a

Fourier transform. A lens does not perform a Fourier transform, the field pattern in the far field can be approximated by the Fourier transform of the field pattern in the pupil plane. A lens merely causes the pattern in far field to occur in the image plane.

2.1.4 Phase Holograms. Thus far, it has been shown that in order to steer a beam, one needs to linearly vary a beam's OPL. In actuality, this is not the only way to steer a beam. Phase holograms have been used experimentally to shape, split, and even steer beams [10, 12]. A phase hologram is based on the Gerchberg-Saxton phase retrieval algorithm.

The phase retrieval algorithm consists of an iterative technique utilized on a computer to develop a phase screen that, when applied in a pupil plane, will produce a predetermined image in the far field. Figure 2.5 gives a graphical representation of the Gerchberg-Saxton phase retrieval algorithm. The algorithm takes as an input a desired field amplitude pattern for the image plane A_D. The first step of the algorithm is to propagate a field in the pupil plane to the image plane by the use of a DFT. The amplitude of the field in the pupil plane, A_C, is considered to be constant due to assumed collimated input. The phase of the pupil plane field, $\psi_r(x, y)$, is simply a random guess for the first propagation to the image plane. In the image plane, the resulting phase, $\psi(u, v)$, is combined with the amplitude of the desired field and then propagated back to the pupil plane by the use of an inverse DFT. Again in the pupil plane, the phase of the field, $\psi(x, y)$, is combined with the required constant pupil plane amplitude. The above process is then repeated for a desired number of iterations or until the optical field in the image plane yields the desired irradiance pattern within a desired degree of accuracy. Steering beams with this type of phase screen is called the Holographic beam steering method.

If the desired image happened to be the image of a beam spot off of the optical axis, then upon iterating on that image with the phase retrieval algorithm, a phase screen would be produced to render the desired image in the far field. When the holographic phase screen is then illuminated by a collimated optical field and propagated

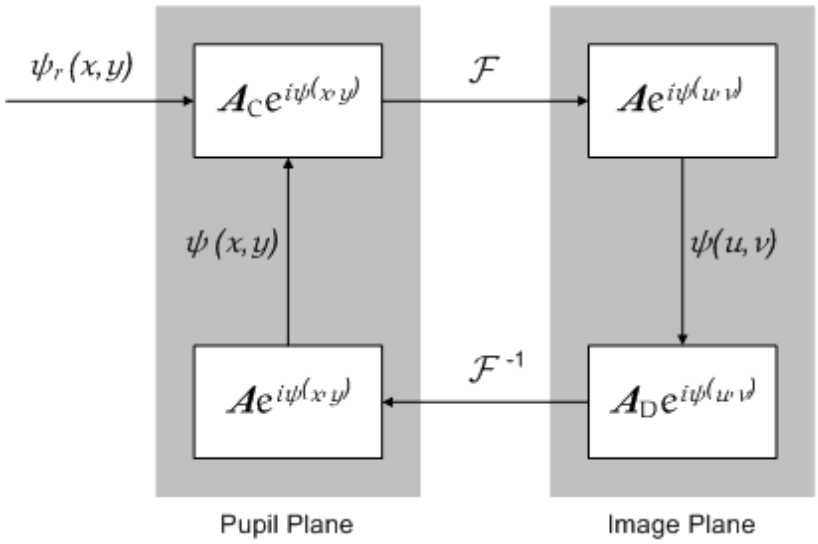

Figure 2.5: The phase retrieval algorithm.

to the far field, the result will be an image of a spot off of the optical axis. Since a collimated field was used to begin with, and an image of an off-axis spot resulted, beam steering occurred. If an image of several spots displaced from the optical axis is used as an input to the algorithm, then multiple beam steering can occur. Implementation of the Holographic method for multiple beam steering will be the primary focus in the chapters to come.

2.2 Simple Mirror

A mirror steers a beam by linearly changing the physical length of the OPL. However, there is a nuance that needs to be mentioned as to the amount of steer angle observed with respect to the delay angle. With a mirror, if the delay angle is θ, then the steer angle will be 2θ. This difference, from what was presented in Subsection 2.1.1, is because, to achieve the physical delay, the normal to the mirror is rotated by θ, as well. For this reason, the actual steer angle that results is twice the delay angle provided. No matter the steer angle, virtually all of the irradiance incident on the mirror face is reflected to the target minus some minor losses due to manufacturing imperfections, as opposed to using blazed gratings which loses power to diffractive orders.

2.3 Spatial Light Modulators

A SLM usually has only a small range in which to apply a phase delay on a beam's OPL. Hence, the steer angle of a SLM is small if applied purely in a continuous linear fashion. A SLM employing a blazed grating can produce a greater phase delay across the wavefront, thus achieving larger steering angles. Unlike a conventional blazed grating which has a fixed steer angle, a SLM can easily change the grating distance, D, in Equation 2.2.

SLMs usually have a segmented or pixellated surface so that an incident beam's OPL can be changed or modulated in differing amounts across the face of the device. If a wavefront encounters different linear phase delays, the beam will be steered to different locations. However, since the face is segmented, the amount of phase delay can be altered in ways other than just linearly. Therefore, SLMs have the ability to cause higher order effects on a beam as well, but beam steering is the focus of this paper so the linear effects are of primary concern.

The number of pixels allocated to each tooth can be increased or decreased, thus changing the steer angle. One must remember that with a pixellated device, the grating will not be smooth and the result will be an increase in the energy lost to the higher orders. Again, this means that the SNR will decrease. The varying blazed gratings are applied on a SLM with the use of phase screens. A SLM can be implemented using different types of technology. Two such technologies use liquid crystals, LC SLMs, and segmented mirrors that are on the scale of micrometers, MEMS.

2.3.1 Liquid Crystal SLM. A LC SLM is a pixellated device that steers a beam by changing the OPL of an incident field through manipulation of the index of refraction encountered [4, 6]. However, the amount of variation in the index of refraction is small so a blazed grating technique is commonly used. A LC SLM changes its index of refraction by using the birefringent properties of liquid crystal. As the liquid crystal is rotated, the index of refraction that an incident beam encounters

varies. The rotation of the liquid crystals is caused by an electric field. As an electric field is rotates, the liquid crystals want to stay aligned with this field so they rotate as well. Figure 2.6 shows a diagram of the rotation due to an electric field and the pixelization of the liquid crystals.

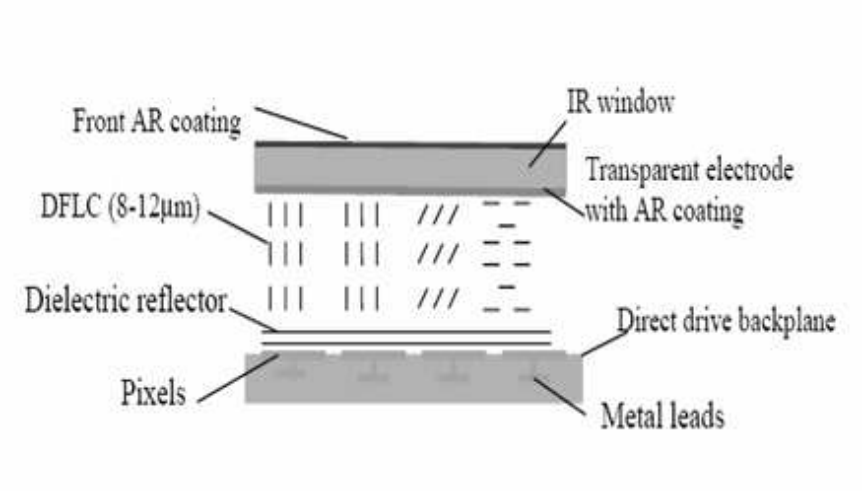

Figure 2.6: Diagram of LC SLM [5].

Figure 2.6 shows that the liquid crystals are not actually segmented, the metal leads (electrodes) behind the pool of liquid crystals cause the pixelization. The sphere of influence of each electrode only affects a portion of the overall pool of liquid crystal. It can also be seen that there is some space between these metal leads. This spacing also causes the issue of fill factor to be dealt with since not all of the liquid crystal can be directly controlled. The uncontrolled portion is influenced by the nearest neighbors influence though. The issue of pixelization and fill factor have effects on the overall phase representation (blazed grating) that can be produced by a LC SLM. Figure 2.7 (a) again shows how a blazed grating imitates a continuous phase modulo 2π. However, a LC SLM can only represent the blazed grating pattern with discrete elements, which is shown in Figure 2.7 (b). The aforementioned fill factor, shown in Figure 2.7 (c), causes the LC SLM's blaze pattern to deviate further from a perfect grating. With discrete elements representing the pattern and a fill factor, the blaze is not perfect which has the effect of lowering the diffraction efficiency for the first order spot.

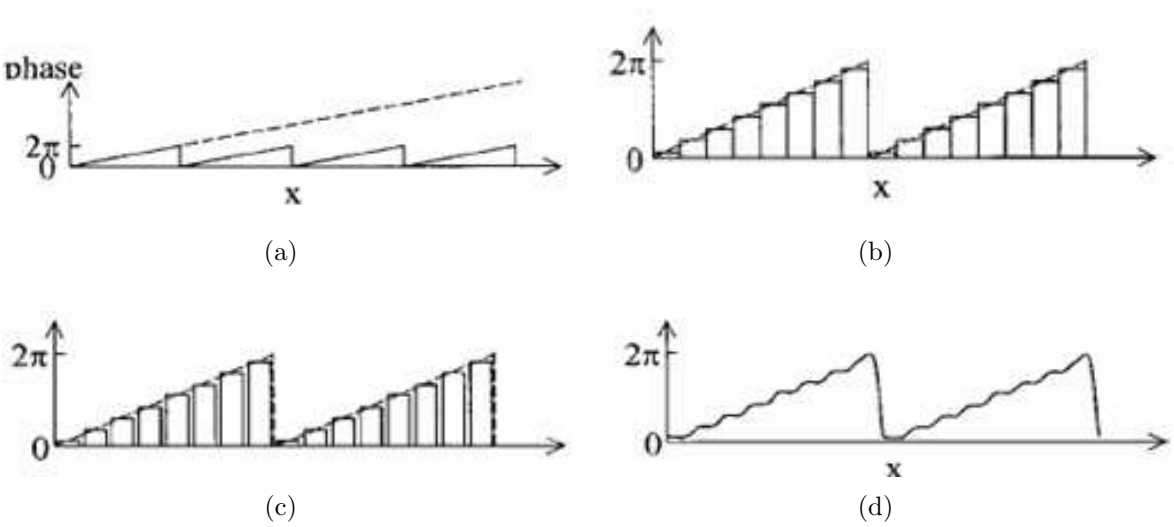

Figure 2.7: (a) Phase delay modulo 2π.(b) Phase delay modulo 2π with discrete elements. (c) Phase delay modulo 2π with discrete elements and fill factor. (d)Resulting phase delay profile from SLM [4].

An electric field cannot be localized to the area of just one pixel. The sphere of influence of each electrode effects the magnitude of the phase delay for the neighboring pixels. [4,7]. This effect is often referred to as crosstalk and results in a flyback region. The flyback region is an inability to get a hard reset after each tooth of the grating pattern. This non-hard reset, as seen in Figure 2.7 (d), further impacts the overall quality of the blazed grating pattern, which again lowers the diffraction efficiency. Crosstalk does have an advantage for the pixels within a respective tooth though. There is an overall smoothing effect which enables each tooth to represent a more continuous blaze, which has the effect of increasing the diffraction efficiency.

2.3.2 Micro Electro-Optical Mechanical SLM. A MEMS device uses an array of small mirrors whose positions are varied in height, which of course changes the physical length of a beam's OPL. The mirrors are also manipulated with an electric field. The actual amount of height change is small, so a MEMS device cannot be used effectively as a beam steering device like a regular mirror, hence the need to steer modulo 2π. The mirrors can be varied independently which produces multiple beam steering capability as well. Figure 2.8 shows a diagram of the construction of

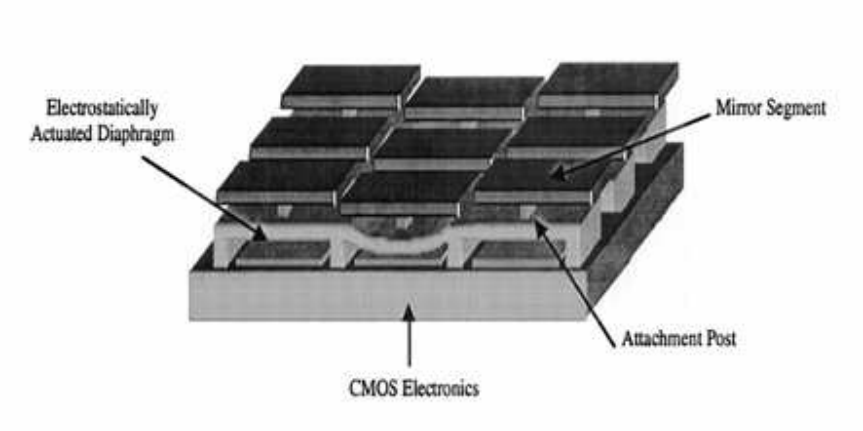

Figure 2.8: Diagram of MEMS SLM [1]

the device. Even though mirrors are employed, the steer angle is not due to $\theta_i = \theta_r$, it is equal to the phase delay angle applied modulo 2π.

2.4 Comparison of Beam Steering Devices

Each steering device has strengths and weaknesses over the other devices. Gimballed mirrors were the only choice for quite some time, however, with the recent advances in SLM technology, designers now have additional choices. The device that is ultimately chosen is often application-specific as there is no one good answer for all needs. A great advantage of mirrors is their large steering angles and that they have proven to be effective over centuries of use.

A drawback of using a gimballed mirror is the fact that it has mechanical parts. Due to inertial resistance, there is a limit to how quickly and precisely the moving parts of the gimbal and mirror can be controlled. To improve response times and precision, the control system needed becomes increasingly expensive and cumbersome. Also, moving parts can make gimballed mirrors impractical for many applications, such as space based systems, due to the harshness of the operating environment and the possibility for the failure of the moving parts in such an environment. A large drawback of a mirror is that "angle in equals angle out." This means a mirror can only steer a beam to one location. Frequently, it is desirable to split and steer an

incident beam to several locations simultaneously. For this reason, a different steering method is needed for multiple beam steering.

SLMs can be an extremely useful alternative for beam steering. They use an electrical field to alter the applied phase delay rather than electro-mechanical means. This use of electrical fields to accomplish beam steering means that high speed steering can be accomplished with very little inertial resistance and power consumption. Since the parts that move with SLMs are on such a small scale, SLMs do not suffer from the drawbacks of a gimballed mirror system.

In most current designs of LC SLMs, the liquid crystals rotate under the application of the electric field to a designated location over a very large range of frequencies. However, they only relax back to their original positions and are not driven by any force other than the force of their internal chemical structure. This relaxation time is slow and makes the overall speed of response for the device fairly slow, on the order of tens of Hz [2]. The slow response time is being addressed with the possible use of dual frequency liquid crystals.

With the addition of other chemicals, the LCs can be forced to react at a different frequency. Since this different frequency can produce rotation in the opposite direction, the LCs can be driven back to a certain position rather just waiting out the relaxation time. With the crystals driven in both directions, the response time increases to around 500 Hz [5]. However, the use of an electric field to rotate the LCs causes other issues of concern.

LC SLM devices benefit from the fact that they usually have a large number of pixels, on the order of 256 x 256 or 512 x 512. This gives LC SLMs a distinct advantage over other technologies. The large number of pixels allows for a high resolution of the phase. The smaller the scale with which one is allowed to control in the spatial domain, the higher the control yielded in the frequency domain. In other words, finer resolution allows for the ability to correct higher frequency aberrations.

The use of birefringent LCs varies the index of refraction but comes at the cost of having a wavelength dependency. Each LC device is designed to work at a specific wavelength and most other wavelengths will not experience the desired effect. However, MEMS SLMs have mirrors that suffer from no such wavelength dependency.

A MEMS SLM's mirrors are moved with a displacement of about 2 μm of stroke and has 2 nm repeatability. Its surface has a highly reflective coating with 4 nm RMS of error per pixel. The maximum steer angle of a MEMS SLM device is on the order of around 10 degrees as opposed to a LC SLM's maximum steer angle of around a half of a degree. The bandwidth of a MEMS device is around 7 kHz which is far higher then an LC SLM, which means phase screens can be applied at a faster rate. The previous device specifications were taken from the Boston Micro Machines website. However, the amount of pixels that MEMS devices come with to date is around 40 x 40 which yields pretty low frequency resolution.

2.5 Summary

In general, beam steering is fairly simple; change the OPL by linearly varying n or l, and a beam can be steered. Fourier analysis gives mathematical relationships between fields at one location with respect to the field values at some other location. Holographic phase screens have changed the conventional thinking on beam steering. A linear phase delay is now not the only way to achieve beam steering. The devices used to create variation in OPL can be simple, as with a mirror, or complicated and high-tech as with SLMs. The method used to steer the beam can vary and is usually determined by current technology and the needs of the specific application. Regardless of which method or device is used, beam steering is still an important area of research.

III. Simulations, Methods, and Setups

Beam steering and optical tracking with SLMs will give the Air Force the capability to implement an optical communications link with no moving parts [11]. A scenario in which such a link would be useful is given in Section 3.1. A means for testing the beam steering theory presented in Chapter 2 using computer simulations is presented in Section 3.2. In Section 3.3, methods for producing linear and holographic phase screens to be used on SLMs for beam steering and tracking are discussed. Before actual work on an optical bench can begin with a SLM, it must be calibrated. The calibration procedure includes a phase to gray conversion and compensation for the backplane warping of the SLM. The calibration process can be found in Section 3.4 along with specifications of SLMs used. The effects of beam steering with a SLM is presented in Section 3.5, which compares the linear and holographic methods. An optical bench setup is described to split and steer a beam with a SLM that will be used with both linear and then holographic phase screens. Once linear and holographic phase screens can be used on a SLM, it is only natural to compare the two techniques. Section 3.5 will offer the results of the comparisons and other effects of beam steering with a SLM. Finally, in Section 3.6, a setup will be given to produce spots of light being steered with linear phase screens which will be tracked using holographic phase screens. This final setup will provide the means to prove the primary goals of this thesis which are beam splitting, steering and tracking and demonstrate that the Tracking method can be used in an optical communications link.

3.1 Communication Scenario

Imagine a Predator unmanned drone being used to optically pass information to several tanks as they move throughout the battlefield. Each tank has a beacon mounted on it and a detector to receive a signal. The Predator has a detector and a device to steer the light signal to multiple targets. As the Predator detects the beacons mounted on the tanks, the steering device is used to subsequently steer the

communication signal to each of the tanks. This is a one-to-many optical communication link and will allow simultaneous transmission of information to multiple receivers with extremely high bandwidth.

As discussed in Chapter 2, there are several methods one could use to steer a beam to each tank. If a mirror is used, one could try to steer at a high rate, delivering packets of information to one tank at a time so as to make each tank think that they have a quasi-continuous link to the drone. However, this would take a robust control system and gimbal to accomplish this type of fast and accurate steering with a mirror. Another option would be to have several gimballed mirrors to simultaneously communicate with multiple tanks. Due to the size and weight constraints of a Predator though, it is obvious that neither of these two options would really be practical.

Another method one could utilize to steer the light is with SLMs. As seen in Chapter 2, they have the ability to split one beam into several. This eliminates the need for multiple mirrors and the robust steering controls. Since a SLM can apply phase screens at 10 Hz - 7 kHz depending on the device used, SLMs can steer fast enough to communicate with a tank on the battlefield. Of course, the principle of the conservation of energy still applies. Each spot will be reduced in energy than a mirror had been used to steer it. If need be, a more powerful laser is easier to add to the Predator than a large steering control system or multiple mirrors. For these reasons, the use of SLMs, in a one-to-many communication link like the Predator-to-tank communication scenario, is a better option than using regular gimballed mirrors.

3.2 Verification of Theory

Chapter 2 gave us the needed theoretical treatment in order to understand beam steering but still is simply a model with which to predict what should occur when a phase screen is used to modulate an optical field. Computer simulations will provide the proof of the theory. Both linear and holographic methods can be tested in simulation, and methods to do just this will be developed in this section.

To verify that beam steering would take place with the application of a linear phase delay applied modulo 2π on a SLM, MATLAB® can be utilized. The process to be modeled with computer simulations begins with a plane wave of unit amplitude incident on a SLM. The field is then phase modulated by the amount of phase delay provided by the each pixel of the SLM. The linear phase delay is applied on the SLM in the form of a phase screen which contains the amount of waves of delay each pixel will apply to the incident field. The modulated field then propagates to the far field where the diffraction pattern can be observed. The image plane matrix that results is the DFT of the SLM but shifted, due to the applied linear phase delay. Development of the beam steering phase screens is the main objective of the computer simulations because that capability will still be utilized even when the computer is no longer being used to model field propagation.

To develop the necessary phase screens, model the SLM, and simulate propagation of the modulated fields to the far field MATLAB® was used. MATLAB® is a matrix based language and it can be used quite effectively to model the pixels of a SLM and pixellated optical fields. Each element of a square matrix, which represents a phase screen is the amount of phase delay the phase screen provides to an incident field. Multiplying a matrix, representing the incoming field, and the applied phase screen will model what happens to the field as it interacts with each pixel of the SLM. The amount of phase delay applied can be varied to allow for different steering angles by changing the elements of the respective phase screen matrix.

As a field emerges from the SLM, it is pixellated and phase modulated. As seen in Chapter 2, the resulting modulated matrix can be propagated to the far field using using a DFT. A matrix containing the result of the DFT of the modulated matrix represents the field in the image plane. The image plane matrix can then be plotted to get a visual representation of the result of the phase modulation. The result will provide verification of beam steering theory. When plotted, the image plane matrix will contain a Sinc pattern with the center lobe, or main spot, steered

to its respective location. The phase modulation that is applied with the use of phase screens is produced using linear and holographic methods.

3.3 Beam Steering Methods

There are three different beam steering methods utilized throughout this experiment. The first method is the Linear method which will use a phase screen to steer a beam to a single location. The second method is the Quadrant method which will use multiple Linear method phase screens to split and steer a beam to multiple locations. The third, and most important method to this research, is the Holographic method. The Holographic method will use a desired image of off-axis spots to steer a beam to multiple locations.

3.3.1 Linear Method. A SLM cannot yield very much continuous phase delay so phase screens that are applied on them must account for that. As mentioned in Chapter 2, a blazed grating is often used to represent a linear phase delay modulo 2π. In MATLAB®, phase screens can be developed to model blazed gratings. Figure 3.1 illustrates an example of a linear phase screen. The steer angle that a phase screen applies to an incident field can be altered by using Equation 3.1, where θ_s is the desired steer angle and A_p is the amplitude of phase delay for each respective pixel of the SLM.

$$A_p = x \tan \theta_s \tag{3.1}$$

If Equation 3.1 is applied on a matrix that represents the pixel's spacing of the SLM, the result is a phase screen that has a continuous linear tilt. The continuous linear tilt is broken up modulo 2π to yield a phase screen of values between 0 and 1, where 0 is no phase applied and 1 is one wave of phase applied.

3.3.2 Quadrant Steering Method. If one wants to steer to several locations simultaneously, several smaller versions of the phase screens developed using the Linear method can be applied on portions of the SLM. In other words, one could develop

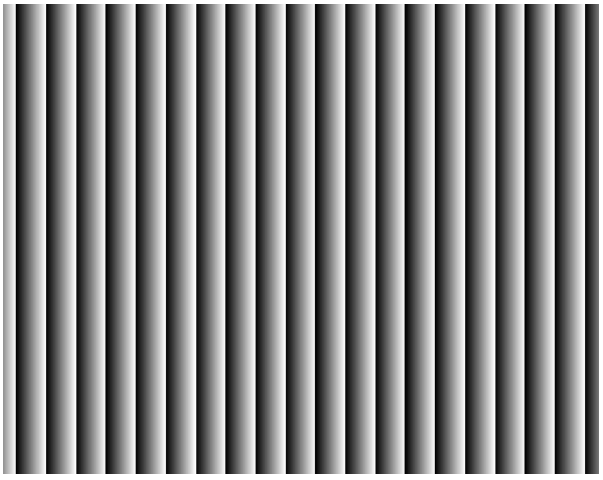

Figure 3.1: Linear phase screen.

linear phase screens to be applied on quadrants of the total number of pixels. Figure 3.2 illustrates the Quadrant method. Since each quadrant has a different blazed grating than the others, each quadrant will steer a portion of the total incoming field to different locations. The Quadrant method splits an incoming beam to yield a multiple beam steering capability.

If the size of the quadrants is altered, then one can shift power between beams [10]. A spot resulting from a quadrant with more SLM real estate will a have higher irradiance than the other spots. This is because a larger portion of the incoming optical field is used to produce the respective spot.

3.3.3 Holographic Method. In Chapter 2, it was mentioned that the Holographic algorithm is based on the Gerchberg-Saxton algorithm where the field amplitude of a desired image is the input. The algorithm produces a phase screen that, when illuminated by an incoming uniform field, yields the desired image in the image plane. It was also discussed that if the desired image is of spots of light off of the optical axis, then multiple beam steering will occur.

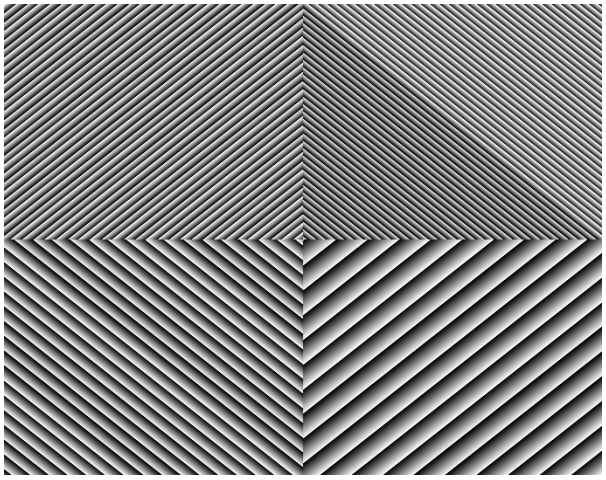

Figure 3.2: Quadrant phase screen.

Figure 3.3 illustrates a realization of a holographic phase screen. This figure is actually a holographic realization of the quadrant phase screen shown in Figure 3.2. The figure is referred to as a holographic realization because the algorithm does not produce exactly the same phase screen each time it is performed. The holographic algorithm starts with a random phase in which to build a phase screen, so the initial conditions are different each time through the algorithm. The resulting image in the image plane is, for the most part, the same each time. One can see that the holographic phase does not look completely random. The phase screen that is produced from a random starting position usually converges to appear much like the linear phase screen that produces the same amount of shift.

In theory, any image that the holographic algorithm is used to iterate upon will have a phase screen developed so that its respective image is reproduced in the image plane. When the desired image is more complicated than an image of a spot, the phase appears more random because the phase pattern needed to create the image is much less predictable. Such a phase screen is shown in Figure 3.4. The resulting images, in the image plane, of all of the phase screens displayed thus far will be shown in Chapter 4. The holographic algorithm has the potential to produce phase screens

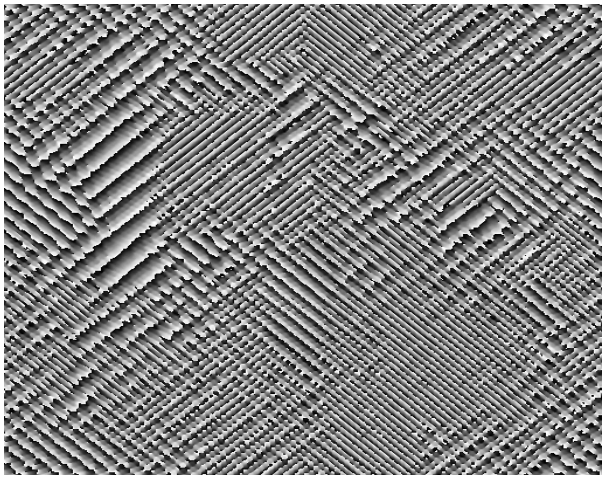

Figure 3.3: Holographic phase screen.

that yield much more complicated images than just spots of light steered off of the optical axis and even images that move in time.

3.3.4 Dynamic Beam Steering. Thus far, only static images of spots being steered off-axis have been discussed. However, if a sequence of phase screens with slightly varying steering angles are produced, then the resulting spot will change position in time. This means dynamic beam steering can occur. The phase screens can be developed using several different techniques with varying effects. Phase screens produced by the Linear method will provide the ability to dynamically steer one spot.

Phase screens produced using the Quadrant and Holographic methods can dynamically steer multiple beams simultaneously. To develop the phase screens for the Quadrant method, four different linear phase delays are used. Each quadrant has a distinct blazed grating that is varied in time and each will steer light to changing positions. To produce dynamic beam steering with the holographic method, a series of images are iterated on that show the same image but shifted slightly to different positions. In other words, iterate on images of moving objects and the algorithm creates phase screens that produce images that move in time.

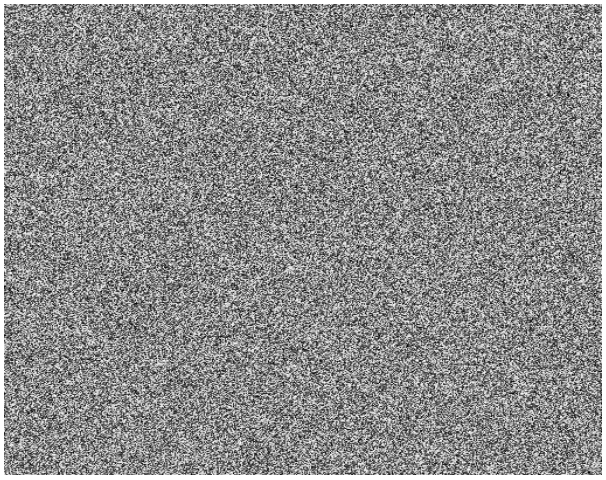

Figure 3.4: Holographic phase screen that yields a complicated image.

3.4 Characterization of the SLM

General specifications on a LC SLM were given in Chapter 2, but the actual SLM and how it will be employed to apply phase screens on an optical bench still needs to be characterized. The specifications given were taken from [2]. The layout on the bench begins with a 2.0 mm HeNe laser emitting light at a wavelength of 632.8 nm. The beam then enters a microscope objective where it is focused down and passes through a spatial filter. After the spatial filter, the beam closely approximates a point source of light emitting spherical wavefronts. The point source is located at the front focal length of a lens which collimates the light. The expanded field then hits the face of the SLM which imparts upon it the desired phase delay. After this point, the setup will change to accommodate three different parts of the experiment. In total, there are four different setups that will be utilized. The first setup presented, which uses a different setup then the one just given, is used for phase to gray calibration of the SLM.

3.4.1 Specifications of the SLMs. To apply phase screens on an optical bench, a LC SLM from Boulder Nonlinear Systems, Inc. is employed. It is a reflective

device that controls phase by changing the index of refraction that is imparted on an incident optical field. The aperture size is 7.68 mm square and has 512 x 512 pixels which means the pixels are 15 μm square. It is designed to operate on a wavelength of 635 nm and can provide a 2π phase stroke. The switching frequency is 10-75 Hz. This determines the refresh rate at which new phase screens can be loaded, and hence new locations to which spots of light are steered. There needs to be space between the pixels for the electronics so this results in some dead space between the pixels where control of the index of refraction is not possible. Due to this dead space, the SLMs used in this experiment have an 83.4 percent fill factor.

In addition to an uncontrollable region within the useable aperture, there is a portion of uncontrolled liquid crystal around the controllable aperture of the SLM as well. When the face of the SLM is completely illuminated, the uncontrolled portion reflects light onto the optical axis since since the light is not phase modulated in any way. This has the effect of putting unwanted irradiance on the optical axis. The problem is easily compensated for with an aperture to limit light from reaching the uncontrolled outer region of the SLM. A circular aperture of 7.0 mm is included before the collimated field reaches the SLM to reduce this unwanted spot of light. With a circular aperture in the optical path, the resulting focused spot will no longer be a Sinc pattern but now an Airy pattern as mentioned in Chapter 2. A second SLM with the same specifications as the one mentioned above, is used in the when doing optical tracking.

3.4.2 Sampling and Spacing. Now that the geometry of the specific SLM has been characterized, several issues need to be dealt with. Propagation of the field that emerges from the SLM, in simulation, is carried out via a DFT. Along with the occurrence of a DFT comes the DFT spacing described in Equation 2.12. Applying this equation for the SLMs to be used results in an image plane spacing of 20.6 μm. In Section 3.3, it was discussed that a matrix would represent the developed phase

screens and the SLM in simulation. The size and spacing of this matrix still needs to be determined.

To properly represent field propagation in simulation, one needs to ensure that the Nyquist sampling theory is satisfied. This means, for optical field sampling, that there cannot be more than a π phase change between pixels. There are two parameters that can be varied to ensure this criteria is met; the size and number of pixels used to represent the field. The pixel spacing in the pupil plane is fixed due to the SLM having a fixed geometry. The only parameter left to vary, to satisfy the Nyquist criteria, is the number of samples used to represent the field. To accomplish this, an appropriately sized matrix must be chosen, and Equation 3.2 is used when determining the number of samples, N, needed to properly represent the field. D_1 and D_2 are the maximum spatial extent of the field in the pupil plane and image plane respectively. The size of the SLM's aperture is 7.68 mm and the detector size is 3.8 mm placed 250 mm away from the SLM. This results in a N = 738 pixels on a side. However, this sized matrix will cause problems in the development of the holographic phase screens, and its application on the SLM.

$$N = \frac{4D_1D_2}{\lambda z} \tag{3.2}$$

The SLM has only 512 pixels on a side. If a phase screen larger than a 512 x 512 is developed, a certain portion of the phase screen must be discarded if it is to be applied on the SLM. Discarding portions of the holographic phase screens can be problematic. The holographic algorithm produces a random phase distribution, so an ability to predict what effects will result to a respective portion of the resulting image would be is impossible. For this reason, even though the sampling theory is not satisfied, a phase screen size of 512 x 512 is maintained.

3.4.3 Phase to Gray Calibration. When using a blazed grating, the phase varies between 0 and 2π or one wave of phase. The pixels of a phase screen are merely numbers between 0 and 1, which is not what the SLM needs to apply a phase screen. The SLM is given an eight bit number per pixel, called a gray value, in which to apply

a desired amount of phase. The gray values that correspond to a certain amount of waves of phase must be calibrated. Due to this calibration, an SLM designed for a wavelength of 635 nm is used with a source of wavelength 632.8 nm. In other words, every setup is going to be slightly different so a universal look up table for gray values is not possible. The specific amount of phase delay for a specific gray should be measured for each setup. All throughout the phase to gray calibration process the gray values that are commanded are applied uniformly for all of the pixels of the SLM. Figure 3.5 shows the setup used for the phase to gray calibration.

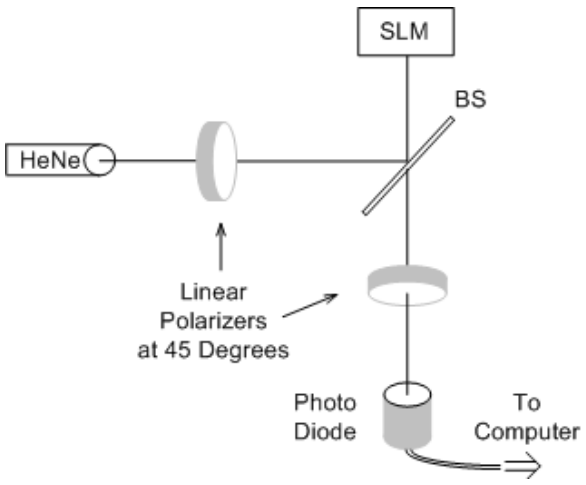

Figure 3.5: Setup for Phase to Gray Calibration.

A field incident on the SLM is polarized at 45 degrees to the extraordinary axis of the liquid crystal by the first polarizer after the laser. This polarization angle is, of course, in the same plane as the face of the SLM. To begin with, the extraordinary axis of the liquid crystal is normal to the face to begin with and the ordinary axis is. Therefore, the incident field is normal to the extraordinary axis and so the field experiences only the ordinary index of refraction, which is just a piston of phase delay and has no effect on the overall polarization of the field. However, when the light reflects off of the backplane of the SLM, the polarization is rotated by 90 degrees. The field is now perpendicular to the second polarizer, so no light passes through to the photo diode.

As the extraordinary axis is rotated the field becomes increasingly elliptically polarized, so there is more of a component of the field that makes it through the second polarizer as the gray value is increased. Equation 3.3 gives the relationship between the irradiance on the photo diode and the phase angle, ϕ, where A and B are constants that depend on the orientation of the polarizers.

$$I(r) = A + B\cos\phi \tag{3.3}$$

It can be seen that the irradiance will start to decrease even though the phase angle is increased when the angle crosses into the right half plane. This means that a wrapped version of the data is collected and must be unwrapped. The unwrapping is not as complicated as phase wrapping in general due to the knowledge that the phase is always increasing because that is what is being commanded through the increasing gray values. The photo diode gives a voltage that is related to the optical power that it detects. An average voltage for each gray value is found, and the results from a calibration are plotted in Figure 3.6 (a). From the data seen in 3.6 (a), the phase to gray values are then found using a Pade fit to the data, which is shown in 3.6 (b).

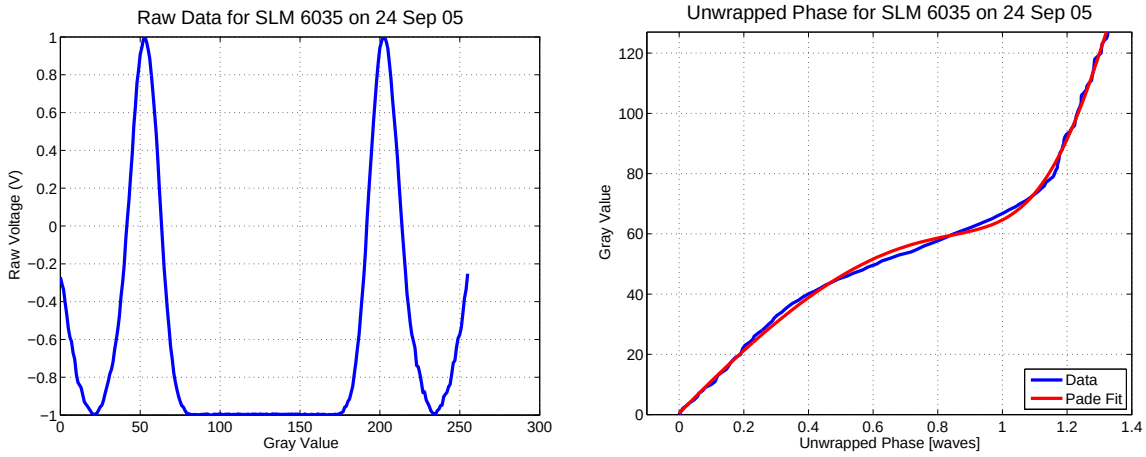

(a) (b)

Figure 3.6: (a) Normalized raw data from the photo diode. (b) Phase to gray fit.

3.4.4 Backplane Compensation. When a flat phase is commanded on the SLM, the theoretical result is an Airy spot as already mentioned. However, when this is done, the result is an aberrated spot of light. This is due to the backplane of the SLM not being exactly flat. A Michelson interferometer, shown in Figure 3.7, and the resulting interferogram is used to characterize the backplane warping of the SLM. A phase screen is developed from a collection of Zernike polynomials that approximates the aberration. Once an approximation of the phase that aberrated the Airy spot is known, then the negative of it can be applied, so the SLM can compensate for its own error. The backplane compensating phase screen is then added to every phase screen in units of waves. The combination is then converted to gray values and a beam steering phase screen is ready to be loaded onto the SLM.

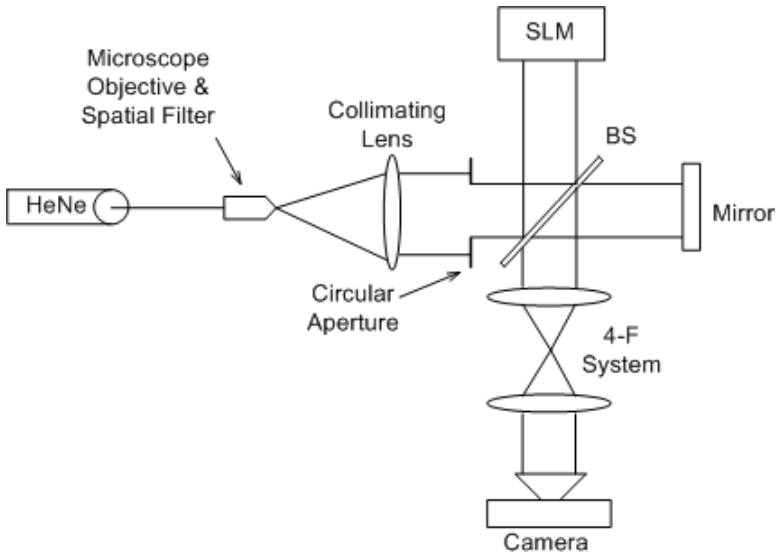

Figure 3.7: A Michelson interferometer is used to correct for backplane warping of the SLM.

3.5 Beam Steering with SLMs

One of the first steps in steering beams with a SLM is to determine the steering limits of the device. The grating equation, Equation 2.2, can be used to determine the amount of shift a beam will experience upon reflecting off of a blazed grating. Hence, the maximum steer angle will be found with the use of the grating equation,

knowledge of the wavelength to be used, and the minimum distance possible for the phase grates. It is a generally accepted rule of thumb that, when working with pixellated LC devices, no less than 8 pixels per phase reset should be used to get good effects. With the conditions of a HeNe laser, 8 pixels per phase tooth, and the SLM having a pixel size of 15μm, the maximum steer angle can be calculated to be

$$\theta_{max} = \sin^{-1}(\frac{\lambda}{8\ pixels}\frac{512\ pixels}{7.68\ mm}) = 5.27\ mrads \tag{3.4}$$

This means that all of the steering must be contained within a radius of 5.27 mrads. Depending on the range involved, this could be a large or small area in which to steer into. Now that the steering limits are known, beam steering is done with a variation of the layout given in the last section.

3.5.1 Beam Steering Layout. Figure 3.8 shows the layout that will be utilized for the beam steering portion of the experiments. The first part of the layout mirrors that which was used for the calibration. The differences in the two layouts begin after the beam splitter where the 4-f system is replaced by one imaging lens. The SLM in Figure 3.8 is used to apply phase screens that cause the incident field to be modulated in the desired way. The phase screens can be produced by either the Linear, Quadrant, or Holographic methods. The lens is followed by a digital camera which is placed at its back focal point to capture images of the steered beams. The camera is a 1280 x 1024 (CCD) array with 7.5 μm square pixels. However, the array produced by the camera will be used in the holographic algorithm, and it has already been established that that the holographic algorithm should develop phase screens that are 512 x 512. Fortunately, the size of the array the camera produces can be reduced to 512 x 512.

3.5.2 Quadrant versus Holographic Steering Methods. The holographic method of beam steering has several advantages over the linear and quadrant methods. With the Quadrant method, the possible spot shape is fixed. The resulting spot

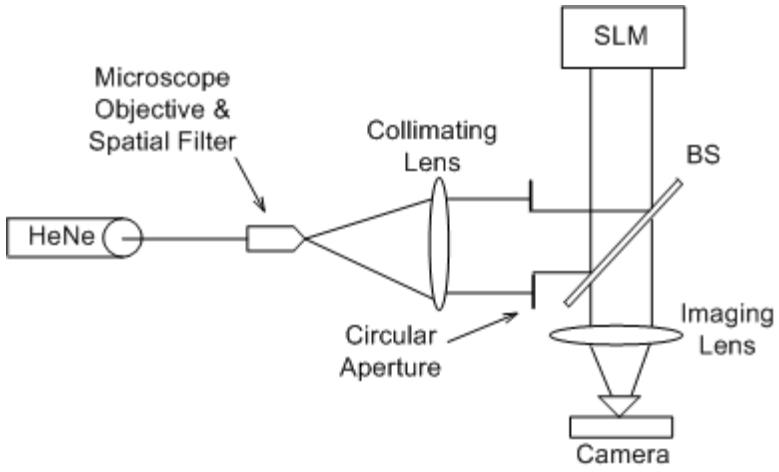

Figure 3.8: Setup on optical bench to use an SLM to beam steer.

shape is determined by the DFT of the geometry of the aperture employed. With the holographic method, any spot shape in a desired image can be provided, as long as a phase screen can reasonably be expected to produce it. That is to say, the phase screen applied on the SLM may simply need too many phase resets to produce the desired shape. The Quadrant method splits the aperture into several smaller apertures. It was shown in Equation 2.11 that the minimum spot size is determined by the aperture size. Hence, the spots produced using the quadrant method, which segments the aperture, will be larger than spots produced by the entire aperture. The holographic method uses the whole aperture to produce each spot so the minimum achievable spot size will be smaller than one could get with the quadrant method. A smaller spot size means that you can get a tighter, and thus a more intense, spot on a target.

3.5.3 Dynamic Beam Steering on an Optical Bench. As discussed in Subsection 3.2.4, phase screens can be generated to produce dynamic beam steering. The phase screens can be applied in sequence on the SLM and the result is an image that moves about the detector's field of view. The steering speed is limited by how fast the SLM can load and apply the respective phase screens. In addition to the method

described in Subsection 3.2.4, there is another method that can provide the ability to move an image using the linear and holographic methods together.

Dynamically steering a spot around using linear and holographic methods combined would not be all that extremely useful. However, if a holographic phase screen is producing a complicated image, then adding successive linear phase screens will cause the image to be shifted by the amount of delay applied by each respective phase screen. For example, say someone wanted to produce an image like Batman's symbol and move it around the night sky. The holographic method could produce the Bat sign, and the linear phase screens would steer it around. Regardless of which method is used, once you can dynamically steer light, the next step is to know where to steer the beams and have some method to track the targets as they move.

3.6 Optical Tracking with SLMs

The power and flexibility of the holographic beam steering method will be exploited to provide holographic optical tracking. The layout differs from the previous beam steering layout only in that another SLM, with similar specifications, has been added to produce a second set of spots simultaneously on the detector. Figure 3.9 shows what this layout looks like on the optical bench. With this setup, it is possible to demonstrate active optical beam tracking on a optical bench in near-real time with the use of two SLMs.

The tracking process described above will provide an open loop tracking ability for the Predator in the previously mentioned communication scenario. The tanks in the purposed scenario have beacons mounted on them to facilitate an ability to track them optically. Obviously, it is impractical to place multiple tanks on an optical bench, so something else must represent them. The Quadrant method is able to produce multiple dynamic spots of light on the detector, so it can provide moving spots playing the part of the tanks. The Quadrant spots in the tracking process will act as the tank's beacons being imaged onto the Predator's detector and will provide the pointing locations to steer to.

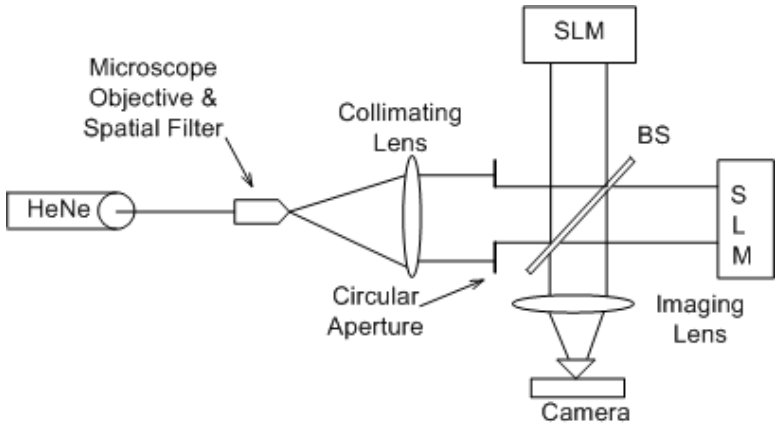

Figure 3.9: Tracking Setup used to display one set of spots being tracked by another set of spots.

Using the images of the positions of the beacons and the holographic tracking algorithm described above, the Predator now has an open loop method in which to track the tanks and subsequently steer light back onto the tanks. The holographic method can simply use the spots produced by the Quadrant method to determine pointing angles to the targets. It is almost as if the Holographic algorithm has potential to act like the eye of a living creature. An animal can see a spot and, in return, point to where the spot is located. The Holographic method will provide this type of capability to the Predator so that it can fly around peering at its prey.

3.7 Summary

Multiple beam steering and tracking offers the ability to communicate with many receivers simultaneously. Computer simulations with the use of MATLAB® provide an effective method to verify beam steering theory. The use of MATLAB® also offers the ability to produce the phase screens to be loaded and applied on an SLM. There were several methods discussed to build the phase screens, which included linear and holographic techniques. Each technique has the ability to split a beam and steer to multiple locations simultaneously. With the use of a detector and the Holographic method, optical steering and tracking can be performed. With optical steering and tracking, a one-to-many communication link may be realized.

IV. Results

This chapter discusses the results of the simulations and experiments conducted during the development of the basic techniques to implement a one-to-many optical communications link. The computer simulations in Section 4.1 will show that linear and holographic phases can steer a beam. It was mentioned in Chapter 3 that the Holographic method can produce more complicated images than just spots of light. In Section 4.2, some images will be shown to illustrate the abilities of the Holographic method in terms of phase screen generation. The results of a comparison of spot quality between the Quadrant and Holographic methods, when used on a SLM, will be provided in Section 4.3. The results of this comparison indicate that a new technique using the Holographic method must be developed in order to make optical tracking feasible. Section 4.4 outlines the development of this new technique, which will make it possible to achieve the communication link.

Most of the images that are shown in this chapter are negatives of the real images produced during experimentation. Some images are computer simulations, produced in MATLAB®, and others are from the detector (CCD camera). Both types of images have been inverted using MATLAB®for printing purposes. If an image is simulated, or from the camera, it will be labeled as such. The MATLAB® code that is used to produce the results in this chapter can be found in Appendix A.

4.1 Computer Simulations

The theory presented in Chapter 2 predicted the effect of a linear delay on a uniform field, that is, the FT of said field results in a spot located off the optical axis. This section will show the results of computer simulations to test this theory. To begin with, single beam steering will be tested with the use of the Linear Method from Chapter 3. After the Linear method, the Quadrant method will be simulated. It should be noted that a circular mask is employed in simulation so theoretically the spot shape is an Airy pattern and not the Sinc pattern that Section 3.2 mentioned. However, the extend of the field in the pupil plane is wide, which yields a small enough

spot in the image plane that the Airy pattern can not be observed. Instead, what will be witnessed in the simulated images is a few pixels will illuminated representing the spot location. Finally, the abilities of the Holographic method will be compared to the claims made in Chapter 3.

4.1.1 Single Beam Steering. To verify the beam steering theory and model beam steering with an SLM in simulation, a phase screen must be developed to apply a blazed grating phase on a uniform field. A phase screen to provide 412 μm of shift in the image plane can be developed, and then computing the DFT of this field will determine the image plane pattern. Producing this amount of shift means the delay angle a phase screen must apply to the input field needs to be determined, which can be accomplished with the grating equation. Upon solving the grating equation for the respective shift, a phase delay angle of 1.6 mrads is required. Figure 4.1 shows the resulting image plane pattern. It is seen that the spot, represented by a few pixels of illumination, has shifted over the respective 412 μm. This amount of shift was chosen because it translates into a shift of 20 image plane pixels. This image proves that the use of a phase screen will indeed steer a beam just as predicted in the theory.

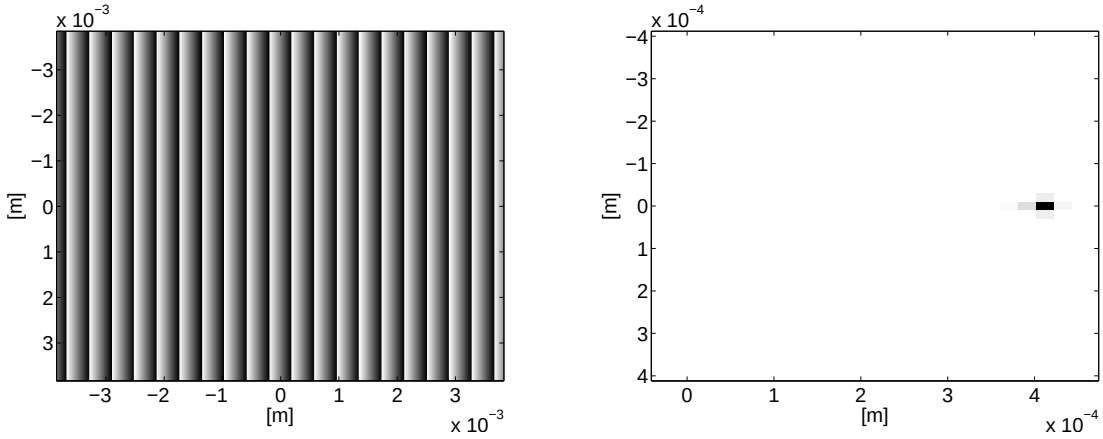

(a) (b)

Figure 4.1: (a) Linear phase screen for 412 μm of shift in the x direction.
(b) Simulation of far field irradiance pattern of the phase screen (a).

The Holographic method uses a desired image on which to iterate in the development of a phase screen to re-create the respective image. Figure 4.2 shows a holographic phase screen that used the image from Figure 4.1 (b) as the desired image on which to iterate. The result is a spot that is steered to the same location as with the application of the Linear phase screen. This type of spot will be referred to as a holographic spot. As stated in Chapter 3, a holographic phase screen is a realization of a random process, since the development of the phase screen begins with random initial conditions. Hence, the phase screen developed should be different each time one is developed as demonstrated in the next section. However, if the holographic algorithm is allowed to iterate long enough on an image that was the result of a simple phase, it will converge to that simple phase pattern. After 100 iterations the holographic algorithm produced the image in Figure 4.2 (a). The holographic phase

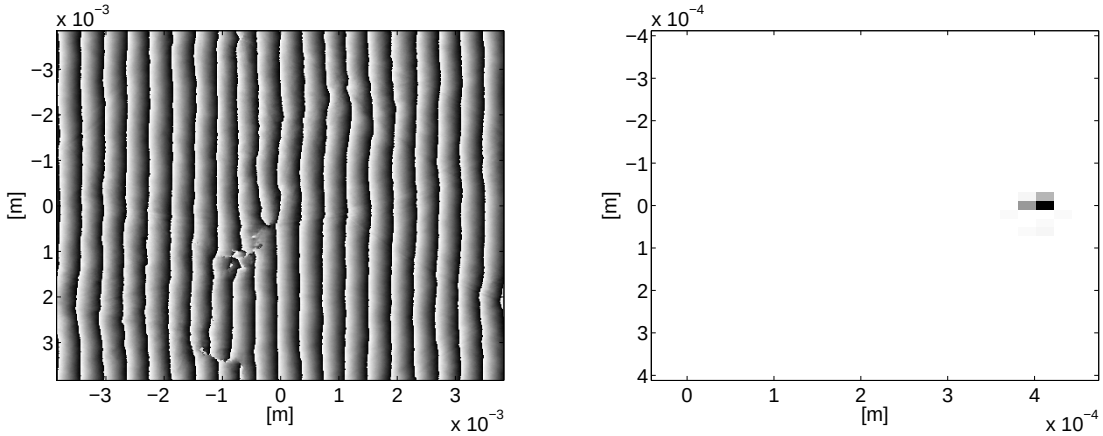

(a) (b)

Figure 4.2: (a) Holographic phase screen for 412 μm of shift in the x Direction. (b) Simulation of far field irradiance pattern of the phase screen in (a).

screen shown is quite similar to the linear phase screen in Figure 4.1. This result gives firm confirmation that the Holographic method is indeed valid and producing correct results. Furthermore, in 4.2 (b), it can be observed that the pixel location of the spot is the same as when a linear phase is used to steer the beam. There is some extra spreading of the irradiance distribution with the holographic phase screen due to the fact that, after 100 iterations, it is still not imitating the linear phase perfectly. Now

that a single beam can be steered in simulation, the next step is to investigate the possibility of multiple beam steering with the Quadrant method.

4.1.2 Multiple Beam Steering. To split and steer a beam to multiple locations, it has been claimed that several smaller linear phase screens combined together as one phase screen would accomplish this task. Such a phase screen is developed using the Quadrant method. With the Quadrant method, the phase screen is segmented into four regions, each containing a different blazed grating pattern. Figure 4.3 shows a simulation of a Quadrant method phase screen to accomplish beam splitting and steering, and its result in the image plane. The original spot shifted 412 μm, (lower left) in Figure 4.3 (b), was retained. The spot is just steered to the left rather than the right as before in Figure 4.1 (b) and is joined by three other spots as predicted. Note that the spots shape will no longer be an Airy pattern with the use of the Quadrant method. This is because there is a circular aperture in front of a segmented square aperture which will result in a shape that looks like $\bigoplus$. The resulting spot shape in the image plane is no longer a standard shape, but nonetheless still appears as a spot of light.

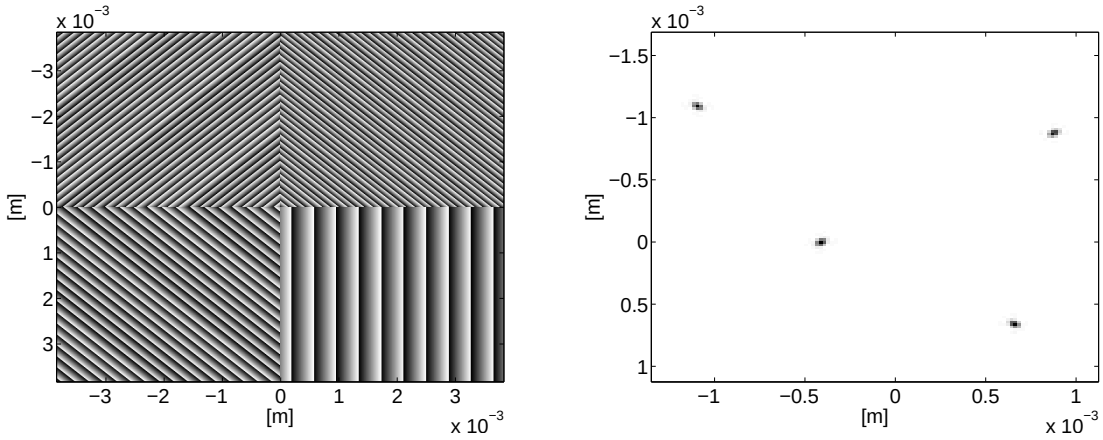

(a) (b)

Figure 4.3: (a) Quadrant method phase screen to produce 4 spots at various steer angles.
(b) Simulated result of the phase screen is 4 spots with different amounts of shift.

Another method of producing multiple beam steering phase screens is to give the Holographic method an image of spots off of the optical axis. After 100 iterations, the Holographic method produced the image in Figure 4.4 (a). It can be seen that the phase screen produced does contain the original linear pattern that shifted a spot to 412μm. Now, this phase pattern shares the phase screen with the differing phase delays that split the incoming beam and steer the other spots to their respective locations shown in Figure 4.3 (b).

Figure 4.4(c) shows a second holographic realization for the image in Figure 4.3. Clearly, the phase screen is different than the previous holographic phase screen shown in Figure 4.4 (a). This is because there are now differing phases that need to be represented by the overall phase screen. There is no specific reason why a certain region of the phase screen would always produce the phase needed for a specific part of an image since it always starts from a random starting point. However, Figure 4.4 (d) shows that the new holographic phase screen still produces an image that has spots in the same locations as the spots in Figures 4.3(b) and 4.4(b). It is observed as well that the two images are not identical. Some spots will end up with more irradiance in a specific realization than the others, but this process will be continually completed as the target spots are tracked so an average amount of irradiance would be deposited on the targets.

4.1.3 Complicated Images and the Holographic method. The Holographic method is theoretically capable of building phase screens which will reproduce almost any image on which it is used. An image of a runway which has a lot of fine contrast changes and sharply defined edges is given as the input to the holographic algorithm. After 100 iterations, the result is shown in Figure 4.5. There is no mistaking that the image is of a runway.

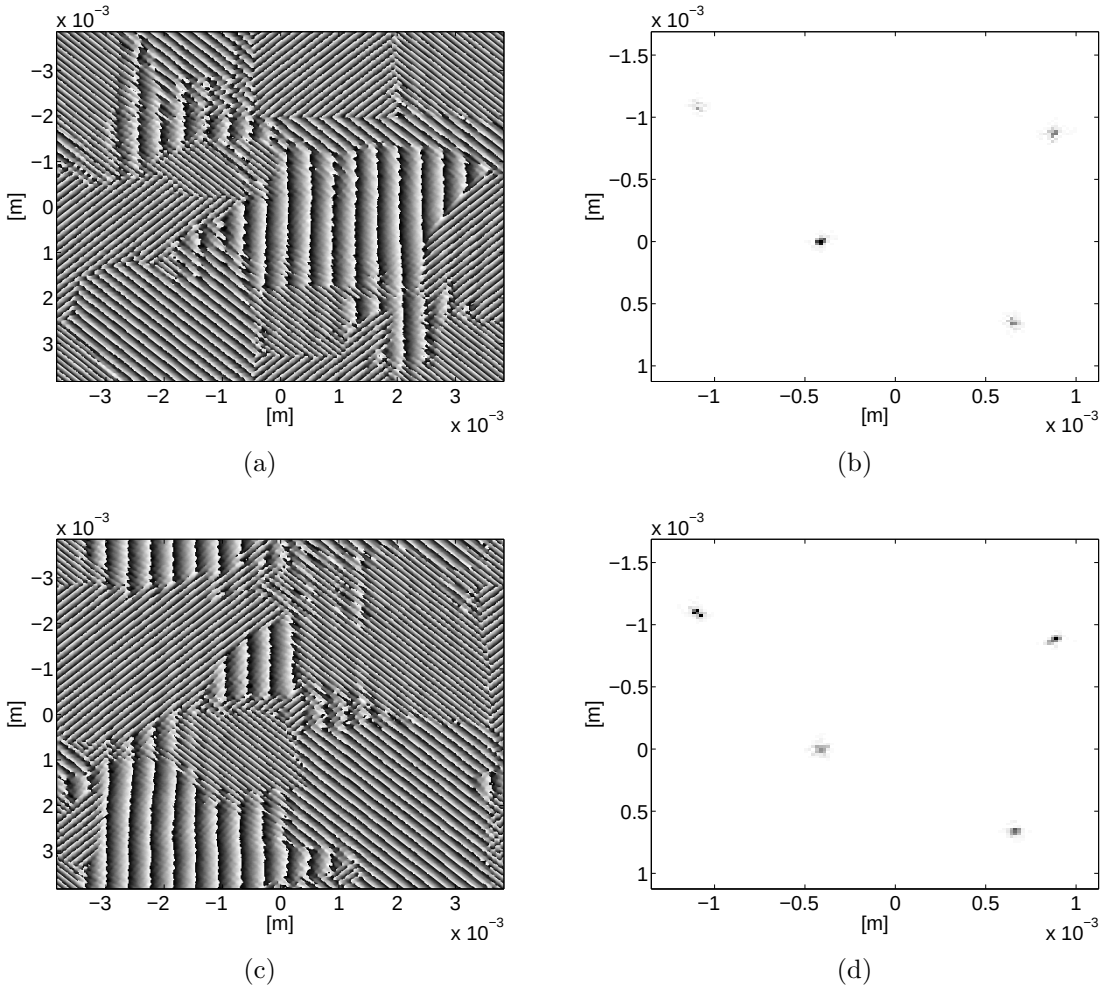

Figure 4.4: (a) Holographic method phase screen of the image in Figure 4.3 (a). (b) Result of phase screen which matches the results from Figure 4.3 (b). (c) Another Holographic method phase screen. (d) The same image is produced as in Figures 4.3 (b) and 4.4 (b).

Figure 4.5: Image of a runway from a holographic phase screen in simulation.

4.2 Beam Steering with a SLM

The beam steering phase screens that were developed in the last section can be loaded onto a SLM to discern if the predictions of the theory and simulation are physically realized. Remember, the holographic phase screens produced thus far are from simulated images of steered spots and not from actual camera images. This fact will come into play soon.

4.2.1 Single Beam Steering with a SLM. The linear and holographic phase screen for 412 μm of shift applied on the SLM is shown in Figure 4.6. Figure 4.6 (a) shows that the spot is shifted over 412 μm. This amount of shift actually shows up on the camera centered about pixel location (312,257) where the center of the image is located at (257,257). This means there was 55 pixels of shift in the image in the camera instead of the 20 pixels of shift the phase screen was designed to yield. This is because the camera has a pixel size of 7.5e-6 μm, and 55 pixels of shift means the same spatial shift occurred as in simulation. This issue of 55 pixels of shift will be

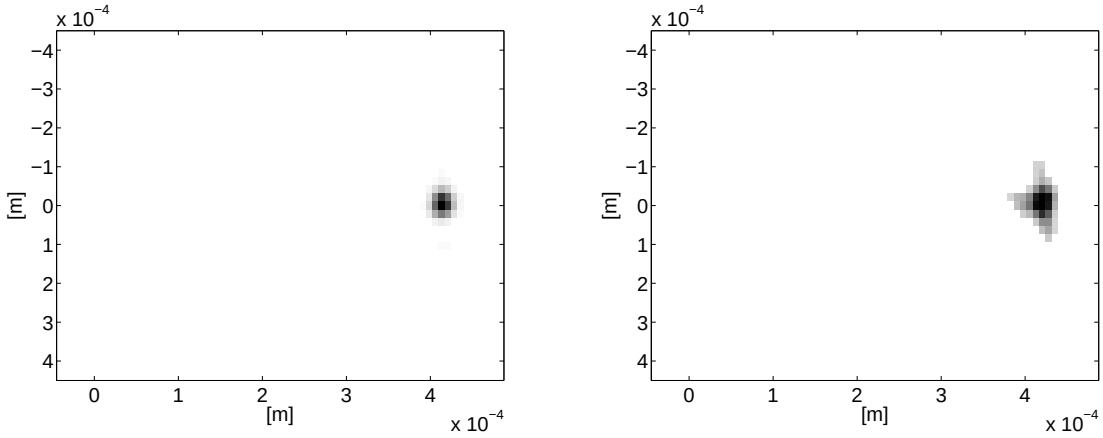

(a) (b)

Figure 4.6: (a) Camera image of the 412 μm-of-shift linear phase screen when applied on the SLM.
(b) Camera image of the 412 μm-of-shift holographic phase screen when applied on the SLM.

needed in Subsection 4.2.1 when the camera image is used as input to the holographic algorithm. The result of applying the holographic phase screen is shown in Figure 4.6 (b). This shows that the Holographic method is physically capable of steering a beam, and it is evident that results are in line with the theory.

4.2.2 Multiple Beam Steering with a SLM. The phase screens that split the incoming beam and steered it to multiple locations in simulation were applied on the SLM and the resulting images are shown in Figure 4.7. It can be seen that the Holographic method spots have more spread to them than do the spots from the Quadrant method. A possible reason for this is that not enough iterations of the holographic algorithm had been carried out in developing the phase screen. However, it is more likely that something more fundamental is to blame. The holographic algorithm is used to imitate spots that have already spread due to propagation, so they are more spread out, as well. This idea of imitating spots after propagation will be revisited in Section 4.4.

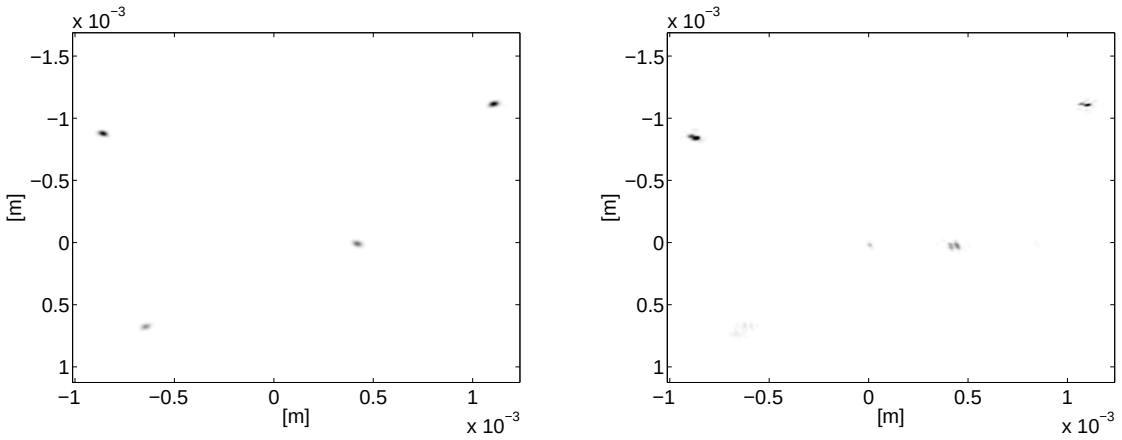

(a) (b)

Figure 4.7: (a) Camera image of a Quadrant method phase screen to produce four spots at various steer angles.
(b) Camera image of a Holographic method phase screen to produce the same four spots as in (a).

4.2.3 Phase Screens that Produce Complicated Images. In the Subsection 4.2.3, the use of holographic phase screens to produce complicated images in simulation was shown to be successful. When the runway phase screen is applied on the SLM, the image can be seen on the camera in the laboratory. However, due to the fact that there are so many is little change in contrast in some parts of the image, the HeNe source and the SLM could not produce the image well enough for it to be printed in this document. However, in Chapter 3, the ability to produce a holographic phase screen that will yield the Bat sign was mentioned. When this phase screen is loaded onto the SLM, the image in Figure 4.8 is the result in the image plane. The large spot of light in the right wing is the center spot of light from the SLM. This is actually an image of the Bat sign shifted over due to the combination of the holographic phase screen and a phase screen with a linear delay as shown in Subsection 4.1.1. When a series of changing linear phase screens are added to the original holographic phase screen, the Bat sign does move about the detector's field of view. This ability could enable the Predator to "summon help" if need be.

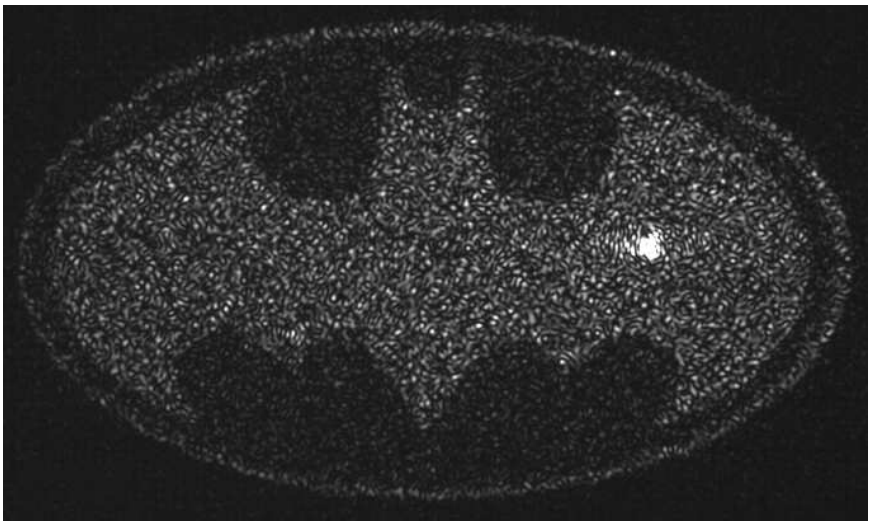

Figure 4.8: Camera image of a phase screen, to produce a complicated image in the image plane, when applied on a SLM.

4.3 Holographic Steering from Camera Images

Admittedly, holographic phase screens developed from simulated images, as performed up to this point, are not really the goal. The detected image from the camera is supposed to be the image that is used to create the holographic phase screens as the communication scenario dictates. To accomplish this step, the camera images are imported into MATLAB® so that the Holographic method can iterate on them. The two-SLM setup, presented in Chapter 3, is used so that linear and holographic spots can be produced on the camera at the same time.

The linear phase screen to produce 412 μm of shift is applied on a SLM, which will be referred to as the linear SLM. The camera image of a steered spot from the linear SLM is sent to the holographic algorithm. A phase screen is developed to produce a holographic spot steered to the same location as the linear spot. Figure 4.9 shows the result when both the holographic and linear spots are displayed on the camera at the same time, where the linear spot is on the left and the holographic spot is on the right. It is obvious from the figure that the holographic spot is not steered to the same location, and has more spread than the linear spot. Prior to this result, the holographic method had performed in simulation as theorized, steering its spot

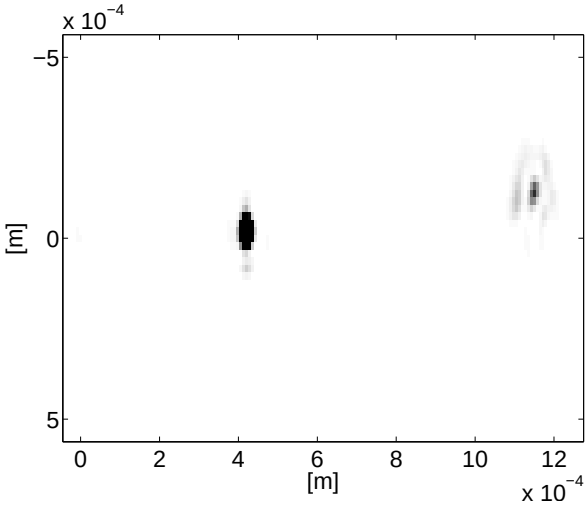

Figure 4.9: Camera image of 412 μm of shift of a linear and holographic spot where the Holographic method used a camera image to build the phase screen. The linear spot is on the left and the holographic spot is on the right.

to the same location as the linear spot. Why, when a camera image is used, do the spot locations no longer match up? This spread in spot size was already somewhat explained previously, but the error in the pointing angle is not the expected result. Upon discovering this result, a first assumption may be that the Holographic method is faulty. However, a deeper look into the details of the method employed and the mathematics behind the physical process is needed if the Holographic method will realize the goal of an optical communications link.

4.4 Improving the Holographic Method

The Holographic method described up to this point, which uses the exact image from the camera, is a misuse of the flexibility of the holographic technique. For example, the spot size of the detected spots will be determined by the diffraction limit of the imaging system used. If the camera image is used to create the holographic spots, the holographic algorithm will produce a phase screen to match the diffracted spot size, which will not yield the smallest spot size achievable from the Holographic method. This effect has already been witnessed in Subsection 4.2.1, in which the

holographic algorithm was used on an image of spots that were already spread out due to a smaller aperture producing them. This means the holographic spots from the Predator would be imitating large spots prior to propagating anywhere and will subsequently spread further upon reaching the targets. This outcome alone mandates the adoption of a different method. As seen from the use of holographic phase screens to produce complicated images, the desired image does not need to be the exact image of the target spots. The desired image can be any arbitrary image.

An arbitrary image can be created that consists of simulated spots. These simulated spots can be much smaller than the detected spot, meaning that the problem of imitating spread out spots with the holographic algorithm can be alleviated. Of course, an arbitrary image that produces a small spot size for the holographic spots is desirable, because the smaller spots will have the effect of raising the SNR of the communications link. What type of arbitrary image will produce the smallest spot size? The first choice that comes to mind is an image with only one pixel illuminated, which will be referred to as the one pixel image. However, the one pixel image has such high frequency content that getting a modulo 2π phase screen to represent it could be difficult. Even though it would be wider than just one pixel, a Gaussian spot may prove to have better results, because a Gaussian spot has gently sloping sides and may possibly be easier to generate on a SLM.

Figures 4.10 shows the application of phase screens on the SLM developed using the holographic algorithm to produce the one pixel image and a Gaussian spot with a standard deviation of one pixel. It is observed that neither spot really produces a difference in size when compared to each other. Both the one pixel spot and the Gaussian spot measured around 8 camera pixels across, where the diffraction limited spot size is 3.3 camera pixels across. However, it is hard to image a spot shape other than the two already experimented with that would yield a smaller spot. Although the one pixel image and Gaussian spot produce similar results, an early selection of the Gaussian spot in the design of this research project dictates that their use is maintained throughout the experimentation. Arbitrary images of Gaussian spots may

produce smaller sized spots on target, but still do not correct for the other and more significant error in the pointing angle.

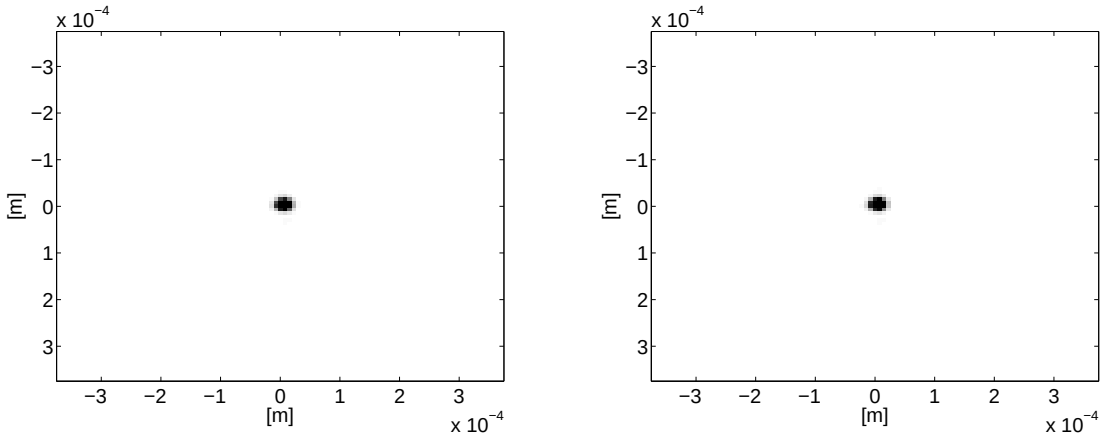

(a) (b)

Figure 4.10: (a)Camera image of the result of the applying the one pixel image phase screen, developed holographically, on the SLM.
(b) Camera image of the result of the applying a Gaussian spot with standard deviation of one phase screen, developed holographically, on the SLM.

Analyzing the actual spot locations could give further insight into what is actually taking place to yield the undesirable spot location. The spot from the linear phase screen is in the same location as the previously shown, but the holographic spot is shifted 1147 μm off of the optical axis. Recall from Subsection 4.1.1, when the phase screen to yield 412 μm of shift was applied on the SLM and a camera image taken, the spot was shifted by 55 pixels. This differed from the 20 pixels of shift the phase screen was designed to yield. Due to the pixel spacing in the camera being smaller than the image plane spacing, it turned out the correct amount of spatial shift was achieved. If the image plane spacing of 20.6 μm and the 55 pixels of camera shift are multiplied together, the result is 1133 μm of shift, which closely matches the observed amount of shift. However, this only answers the question of how the difference in shift can be accounted for as the actual cause is not yet known. For now, a convenient and often used technique of simply blaming MATLAB® can be employed.

When MATLAB® performs a DFT on a matrix, the physical pixel spacing does not matter, a standard pixel spacing of one is utilized. It is up to the user to keep track of the physical spacing. The holographic algorithm is taking in an image from the camera that has a certain amount of pixels of shift and begins performing a forward and inverse DFT on the image to develop the phase screen. The amount of 55 pixels of shift that results in the matrix that the camera provided to MATLAB® is the only thing that matters at this point. The algorithm then produces a phase screen that will yield 55 pixels of shift due to the spacing of that is used, so the angle at which the beam is steered to is incorrect. When the phase screen is applied on the SLM, which has an image plane pixel spacing of 20.6 μm, the result is 1147 μm of shift due to the incorrect steering angle applied. The amount of shift that actually occurs is physically realized in image plane pixels not the desired camera pixels of shift. It turns out that MATLAB® is not at fault, only the method in which it was employed was faulty.

It has already been determined that an arbitrary image of Gaussian spots should be utilized to achieve a smaller spot size, their placement in the image can be arbitrary as well. The Holographic method can be modified to include a correcting algorithm to deal with the problems described thus far. This correcting algorithm first needs to search for the locations of the spots with respect to the optic axis. A fully developed spot locating algorithm that can locate multiple spots in a single image is not the focus of this research, so some constraints are made to the overall process to make the searching process easier. In the Holographic tracking method soon to be demonstrated, each of the four target spots are only allowed to move through out one respective quadrant of the image plane. This allows the correcting algorithm to segment the image into four quadrants and find the location of the spot in each quadrant. Then, to locate the spot, the max command in MATLAB®is used to detect the maximum irradiance. This method works on the assumption that the highest pixel value will be a good representation of where the spot is located. Other methods of locating the spot were experimented with such as centroid location. However, when

calculating the centroid, the background irradiance gave erroneous results of where the spot was located. Thresholding the image could be performed to filter out the background irradiance, but then a method would need to be determined to pick a proper threshold value. This threshold value would need to change dynamically, since the amount of irradiance from each target can vary with range to the Predator, angle to the detector, background irradiance, and atmospheric considerations. This is certainly not impossible or even that difficult, but searching for the maximum irradiance is simpler for the little difference to be gained in spot placement by calculating the location of a spot's centroid.

It turns out the solution to the shift error is quite a simple one with the use of Equation 4.1. When the max command in MATLAB® is used to locate the spot in a quadrant, the result is the pixel location in which the maximum was found. This pixel coordinate, D_{shift}, corresponds to the amount of pixels-of-shift observed by the camera. Now that this is known, a conversion from camera pixel size, P_{cam}, to image plane pixels, P_{im}, is needed. This is due to the fact that the image on which the holographic algorithm is used must have the correct amount of shift in pixels, because of the way MATLAB® computes the DFT with the pixel spacing as discussed previously.

$$N_{loc} = D_{shift} * \frac{P_{cam}}{P_{img}} \tag{4.1}$$

N_{loc} marks the new location, in pixels, where the Gaussian spots should be located in the arbitrary image. Sometimes simple things can be hard to explain, so this equation can be employed on the 412 μm of shift discussed through out this chapter to illustrate its effectiveness. The camera showed 55 pixels of shift, but each pixel is 7.5 μm. The amount of shift needs to be in terms of image plane pixels, which is 20, to yield the correct amount of physical shift when the phase screen is applied on the SLM.

$$N_{loc} = 55\ pixels * (\frac{7.5\mu m}{20.6\mu m}) \simeq 20$$

Once the new pixel location is known, an image of the Gaussian spots can be produced for the holographic algorithm to iterate on. A phase screen is then developed so that the beams can be steered to their respective targets.

4.5 Spot Size Comparison

In Chapter 3, it was claimed that the Holographic method would produce smaller spots. This is due to the fact that Quadrant segments the aperture into smaller apertures and the Holographic algorithm uses the entire aperture to produce each spot. To begin with, to get a larger spot size for comparison purposes, the lens can be replaced with a longer focal length lens to move the image plane further away allowing the spots to spread. In doing this, the difference in spot size will be become more noticeable since in the previous setup the spots are fairly small. Figure 4.11 (c) and (d) gives the result of plotting a cross section of the top two linear and holographic spots in Figure 4.11 (a) and (b). It can be seen that indeed the holographic spots are smaller than the spots produced form the Quadrant method. Also, witnessed in Figure 4.11 (d), the peak irradiance of each holographic spot is higher than the spots from the Quadrant method. It may be more useful to consider the integrated intensity of each spot, but the need for that would be application specific. The size difference between the the two sets of spots will only grow larger if more spots are produced.

4.6 Holographic Tracking and Steering Using an SLM

Now that the Holographic method has been improved with the use of the correcting algorithm to yield the correct spot placement, the problem of tracking spots as the move can be addressed. Again, the Quadrant method, applied on one SLM, will provide dynamic spots that represent the beacons on the tanks as the tanks move around on the ground. The Holographic method begins with the detection of the spots on the camera. Then, the correcting algorithm will identify the location of the spots and adjust for the difference in pixel size between the camera and the SLM. The correcting algorithm will then place one radial pixel width Gaussian spots at

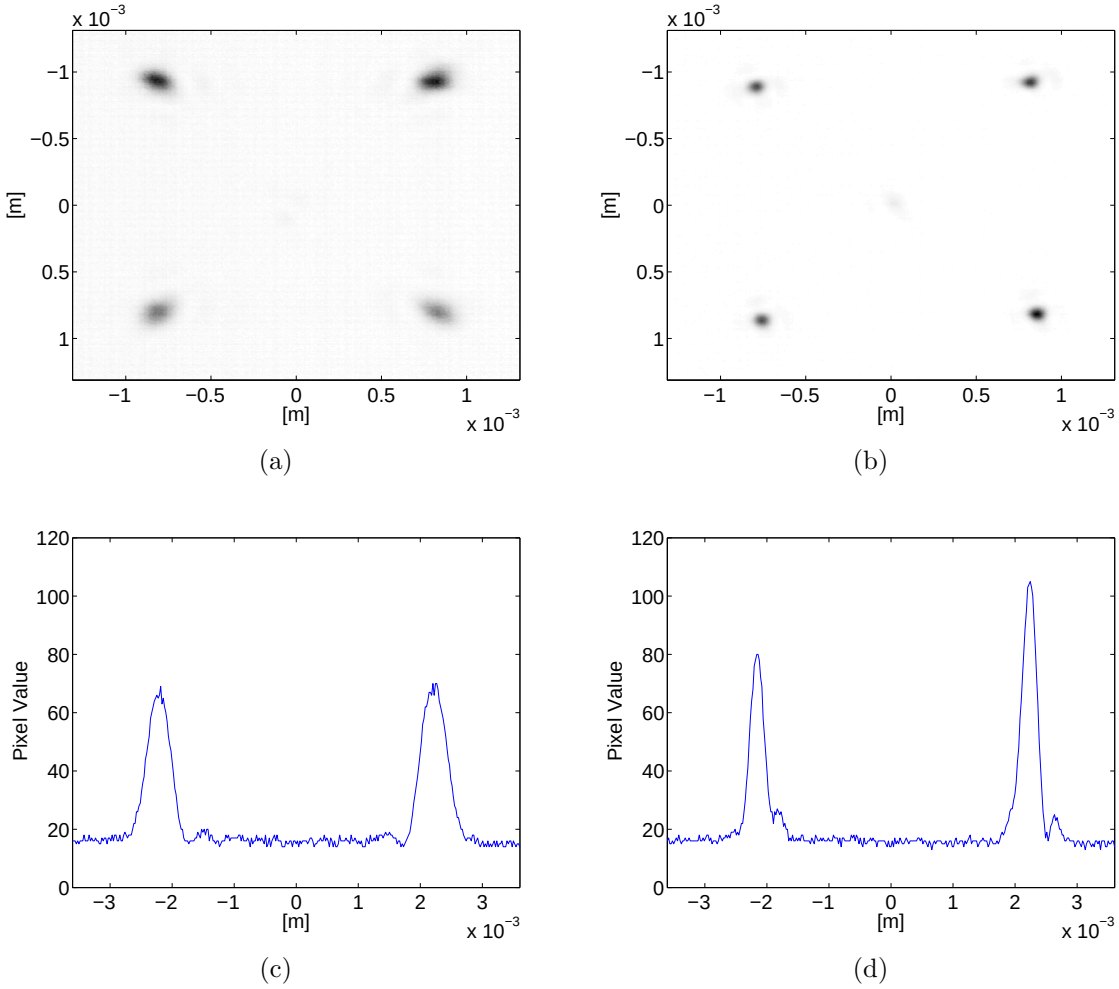

Figure 4.11: Camera image of a Quadrant method phase screen to produce four spots. (b) Camera image of a Holographic method phase screen to produce the same four spots.(a) Cross section of the top row of spots from Figure 4.11 (c) produced by the Quadrant method. (d) Cross Section of the top row of spots in Figure 4.11 (b) produced by the holographic method.

each respective spot location, and send this new arbitrary image to the holographic algorithm. The holographic algorithm then iterates on the image and applies it on a second SLM. Both sets of spots are produced on the detector at the same time so they can be shown to move lockstep together, thus proving that holographic optical tracking is achieved.

Ideally, the method previously described is how the Holographic Tracking method should work. In reality, more equipment limitations prohibit such smooth operation of the optical tracking. The holographic spots are steered onto the same detector as the Quadrant spots to prove tracking is occurring. This means if an image is taken it will contain the holographic spots as well. If the image with all of the spots is sent to the holographic algorithm, it would produce a phase screen that reproduces all of the spots including the detected holographic spots. For this reason an extra step is added to the process which involves commanding the holographic SLM to zero phase so that the field is steered to the center of the image. A mask is then placed over the center 32 pixels to block out the light from the holographic SLM in the detected image before it is sent to the correcting algorithm. This has the effect of slowing the response time of the tracking algorithm. Further slowing the process is the fact that once the target spots have moved, human intervention is needed to actually acquire an image with from the camera.

The time needed to compute a holographic phase screen can be quite costly to the tracking response time. Results of the previous holographic phase screens shown were done with 100 iterations of the holographic algorithm. However, 100 iterations (two DFTs each) takes 78.12 seconds, which takes far too much time to be used in an actual system. In order to cut down on the amount of time needed, a smaller number of iterations can be experimented with. The holographic multiple beam steering phase screen presented above was re-computed with 25 iterations and one iteration. Figure 4.12 shows the result. To do 25 iterations, the time needed is 18.80 seconds which is still too long for practical application. One iteration takes 1.21 seconds, a somewhat more reasonable amount of time. It can be seen that there is no difference in spot size

with the use of one iteration to build the holographic phase screen, for the reduction in response time that it offers. For this reason, the tracking loops shown below are conducted with one iteration to develop each phase screen.

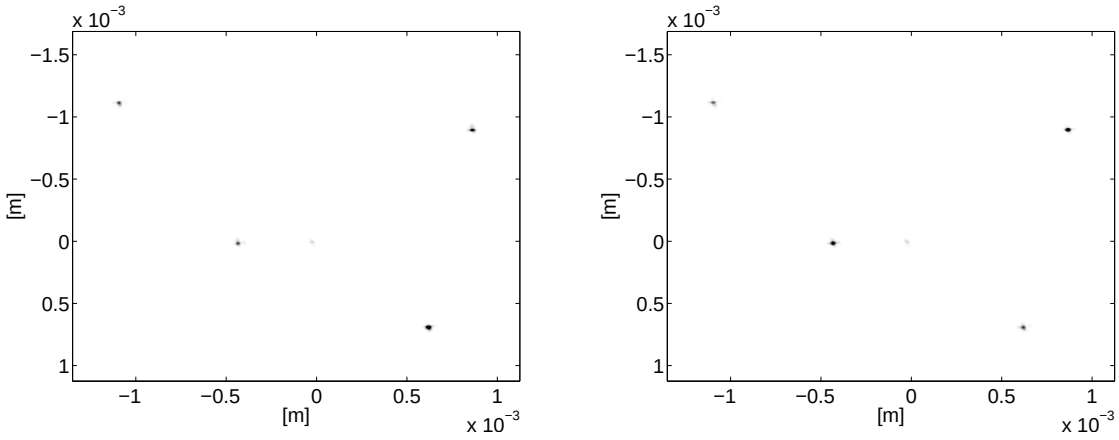

Figure 4.12: (a) Camera image of the holographic spots with 25 iterations. (b) Camera image of the holographic spots with one iteration.

Figures 4.13 show four frames from a tracking sequence. The spot in the upper left moves in a square pattern in a counterclockwise manner. The spot in the upper right hand corner remains stationary. The lower right hand spot moves clockwise it the pattern of a diamond. The lower left hand spot moves in a slow, progressive arc. For the most part, it looks like there is only one set of spots in each frame, because the linear and holographic spots are at the same location. Upon close examination it is possible to resolve two distinct spots at some locations. These instances are where the Holographic method did not steer the holographic spot perfectly on the target spot.

4.7 Summary

The holographic phase screens can indeed split and steer light just as with the application of the more developed method of using linear phase screens. The use of arbitrary images can achieve a smaller holographic spot than if the true detected images are used, and beam steering with holographic phase screens proved to yield

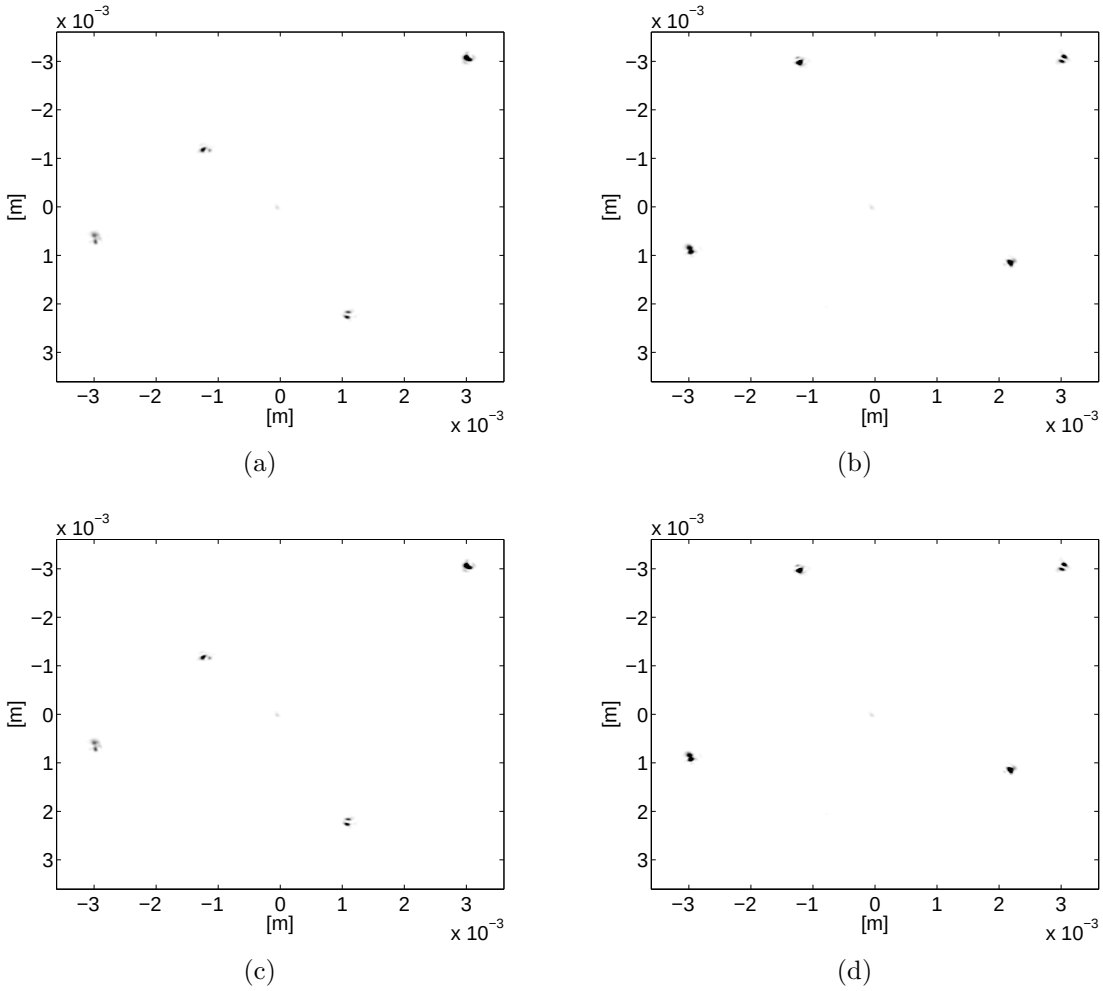

Figure 4.13: (a) Camera image of the holographic spots tracking the target spots (linear spots). This is the first frame of the tracking loop. (b) Second frame of tracking loop (c) Third frame of tracking loop. (d) Fourth frame of tracking loop.

smaller spot sizes than the linear phase screens, as well. If the detector pixel spacing is different then the pixel spacing of the SLM, problems will result in the pointing angle that the holographic algorithm provides. This meant that when the DFT of the desired image was computed, the resulting amount of shift in pixels did not match up. A simple pixel spacing conversion can correct the error in pointing angle that resulted from a difference in pixel spacing. The bottom line is, if the SLM and camera have the same pixel spacing then there is no need to correct for pixel size differences. Optical tracking was demonstrated with some modifications to the Holographic method. These modifications include the use of arbitrary images, the correcting algorithm, and the restriction of the target spots to a respective quadrant. It must be kept in mind, the need for constraining the target spots to a specific quadrant was due to the lack of a fully developed spot locating algorithm and not the Holographic method. Despite the equipment deficiencies, the Holographic tracking method proved to have the capability to track dynamic targets.

V. Implications

Thus far, it has been demonstrated that the Holographic method can be used to track multiple targets and subsequently steer light to them. Section 5.1 will finalize the conclusions drawn from the research completed. A discussion of the issues to be dealt with in realizing the communication scenario, from a systems development perspective, will be presented in Section 5.2. Also, Section 5.2 will offer several new topics to "steer" the interested reader in new directions for future work in developing this important and innovative line of research.

5.1 Conclusions

Beam steering with SLMs is an alternative, and potentially superior, method to the use of gimballed mirrors. For the size, weight, and power consumption offered by SLMs, the steering speeds achievable are much higher than with a mirror and there are no moving parts that may be subject to malfunction. Furthermore, the Holographic method of beam steering offers more flexibility than the Quadrant method because of the ability to spot shape. In addition, the Quadrant method segments the aperture into smaller apertures and the Holographic method uses the whole aperture to produce all of the spots. This means the Holographic method can achieve a smaller spot size, which has the possible effect of raising the SNR of a communications link. With the Quadrant method, to track additional targets that appear in the detector, the geometry of the development of the phase screens would need to be changed to accommodate the extra targets. An additional effect would be an increase in all of the spots due to further segmentation of the SLM's aperture. The Holographic method can easily adjust to more targets without changing how the phase screens are developed, and do it in such a way that does not affect the spot size.

As demonstrated in Chapter 4, the Holographic method put a higher peak irradiance and smaller sized spot on the targets than the Quadrant method with one only iteration of the Gerchberg-Saxton algorithm. This means that the time required to perform one tracking loop is decreased due to the reduced time needed for additional

DFTs to take place. The equipment available prohibited a test of the actual response time between the movement of the target spot and the holographic spot subsequently being steered back onto the target. The maximum tracking and steering bandwidth realized with the current setup and equipment was around 0.25 Hz. The limiting factors in overall achievable response time were due to the lack of ability to quickly perform perform the DFT, the need to command the SLM to a phase of zero before an image was taken, and the fact that human intervention was needed to capture an image. The need to command the phase to zero for the holographic SLM was purely due to the setup of the experiment, and the issue of human intervention can easily be corrected for with a different camera that offers better control of operation.

Overall the tracking loop has two main bottlenecks to contend with, the refresh rate of the SLM and the time it takes to perform a DFT. With the implmentation of a FFT DSP chip, the required DFTs can be accomplished on the order of 100 Hz, so for the time being it is assumed the DFT computation time is not the limiting factor. The current SLM can apply phase screens on the order of tens of Hz. This refresh rate certainly could be the limiting factor of the rate at which the tracking loop is accomplished. With an assumed altitude of 5 km for the Predator, a 20 cm telescope for focusing, a wavelength of 632.8 μm, the resulting diffraction-limited spot size would be around 3.9 cm. Assuming an average refresh rate of 50 Hz for the SLM, and a 20 cm detector on a tank, the tracking loop could track and steer light to a tank moving at 22 mph.

5.2 Discussion and Future Work

Due to the small steer angle of the current SLMs, they probably will not be practical for use in and of themselves for beam steering. Of course, if a SLM is combined with a gimballed control system, as discussed with the use of a mirror, the two systems can achieve much greater beam steering angles. The control system needed would be much less robust than ones used to control a mirror. This is due to

the fact that the control system would only need to change the field of view of the SLM and need not be bothered with actual spot location accuracy.

It was observed from the results in Chapter 4 that the accuracy of the Holographic tracking was not perfect. A correcting algorithm was developed to compensate for the differences in image and camera pixel spacing by adjusting the positioning of spots in an arbitrary image. The spots were slightly off due to the difference in the image plane spacing and the pixel spacing in the detector. Most of the error can be accounted for with the fact that the image plane spacing is coarser than the size of the camera pixels. Hence, the algorithm could not produce the exact amount of shift needed to align as closely as possible. Nonetheless, if the spots are off their mark, the correcting algorithm can be utilized to give a dynamic offset to the placement of each spot so that any pointing errors can be adjusted for if the system had some means of feedback.

The application of phase screens, on the SLM utilized, allowed a target tracking limit of 22 mph, which is not fast enough for practical use. However, the use of DFLC SLMs and MEMS SLMs mentioned in Chapter 2 would certainly enable faster steering speeds. The DFLC SLMs refresh at hundreds of Hz and MEMS SLMs can refresh at kHz and in so doing would make the DFT computation time the limiting factor once again. Of course, the FFT DSP chips could always be employed in some parallel fashion to reduce the time needed to perform a DFT. In essence, if the tracking loop must be performed faster, better equipment is available to allow for tracking of many practical targets.

Instead of beacons, the tanks could be equipped with retro reflectors. With retro reflectors, the illumination that the Predator uses for its desired images in the Holographic method would actually be provided from its own source. The use of retro reflectors would provide the aforementioned feedback needed for the correcting algorithm to adjust for any pointing errors that might occur. The use of retro reflectors would have a further advantage of not using beacons that could make the

receiver easily visible to the enemy. Their use would have the possible disadvantage of allowing the enemy to employ their own reflector and start picking up transmissions. Adding some security measures to the communication signal can combat this particular disadvantage.

The number of targets in this experiment was chosen arbitrarily. In theory, any number of targets in the field of view can be tracked and steered to simultaneously with the Holographic method. Future work should investigate the possible issues that may be encountered when trying to steer to more than four targets. The most likely result is that the SNR would drop, but a more powerful laser could be employed to compensate for the loss in SNR. Additional targets will not affect the refresh rate because the rate at which the phase screens must be applied depends solely on the maximum speed of the targets.

The phase screens applied on a SLM need not be purely for beam steering as mentioned thus far. There is work being done on using SLMs for adaptive optics, as well [9]. Atmospheric turbulence is going to be a major factor for an actual system in the field. Since phase effects are a linear operation on an optical field, a phase screen to steer a beam can be added to a phase screen correcting for the atmospheric turbulence and then applied on the SLM. This effect would require a higher refresh rate for the phase screens because the needed rate would no longer be determined by the speed of the targets but the speed at which the turbulence of the atmosphere is changing. The SLMs used in this research do not have a sufficient refresh rate to accomplish this in the presence of strong turbulence, but again perhaps with a MEMS device atmospheric correction could take place. With the addition of adaptive optics, application of the corrective measures provided above, and the use of methods developed in this thesis, active optical tracking with SLMs can be implemented by the Air Force to realize a one to many optical communications link.

Appendix A. Beam Steering and Tracking Code

This appendix includes the code that was used through the development of the research.

A.1 Beam Steering in Simulation

```
%BEAM STEERING WITH LINEAR AND HOLOGRAPHIC PHASE SCREENS IN SIMULATION
%2d Lt Mawhorter
%Thesis research

% This m_file calls several scripts to develop phase screens for beam
% steering. In the first part of this script, Linear and Quadrant method
% phase screens are produced with a desired steer angle. Then the images
% produced by the phase screens are then used as the desired images to
% generate holographic phase screens.
% This script is the main script used in developing all of the computer
% simulations

clc;clear;

%%% Constants %%%
lambda = 632.8e-9;            %wave length of HeNe laser
k      = 2*pi/lambda;         %wave number
f      = .250;                %m focal length
N_slm  = 512;                 %number of pixels in SLM device
N_img  = N_slm*2;             %used when zero padding
sz_SLM = 7.68e-3;             %physical size of the slm
ds     = sz_SLM/N_slm;        %differential spatial distance
df     = lambda*f/(N_slm*ds); %differential frequency
```

```
max_iteration=[20 50 100 250 500]; %maximum iterations allowed

[x,y]  = meshgrid((-N_slm/2:N_slm/2-1)*ds); [u,v]  =
meshgrid((-N_slm/2:N_slm/2-1)*df);
x_plot = x(257,:);   %used to get physical dimensions on images
u_plot = u(257,:);

%%%the auto feature allows the sequence to be run without any of the
%%%questions that are asked along the way.
auto   = input('Would You Like to Run on Auto? 0 No / 1 Yes / 2
Full->'); if auto == 2
    disp('Don''t forget to set the variables to be saved');
    pause;
end tic;


%%%%%%%%%%%%%%%%%%  Linear Phase screen Development  %%%%%%%%%%%%%%%%%%%%%
% % % to get one spot specify one steer angle
%x_angle  = [.30208]; %steering limit angle
x_angle   = [-.094];  %angle single beam steering images are produce from
y_angle   = [0];
%[x_angle,y_angle] = create_angles(.094,180); %moves spots in spcefied arc

% % % to get four spots specify four steer angles
% x_angle = [-.20 .25 -.15  .094]';
% y_angle = [ .20 .25 -.15   0]';

q_PhScrn  = q_steer(x_angle,y_angle,size(x_angle,1));\\
%U_d is the desired image\\
```

```
U_d       = PhScrn_view(q_PhScrn,auto,2,x,y,'circ',7e-3);


%%%%%%%%%%%%%%%%%%%%%%%%%%%%%  Holographic  %%%%%%%%%%%%%%%%%%%%%%%%%%%%%
h_PhScrn  = h_steer(U_d,max_iteration(3),auto); U_h     =
PhScrn_view(h_PhScrn,auto,2,x,y,'circ',7e-3);


%%%%%%%%%%%%%%%%%%%%%%%%%%%%%  Display Results %%%%%%%%%%%%%%%%%%%%%%%%%%%%%
% figure(1)
% imagesc(u_plot,u_plot,abs(U_d).^2)
%
% figure(2)
% imagesc(u_plot,u_plot,abs(U_h).^2)
% end

figure(1) imagesc(x_plot,x_plot,h_PhScrn) colormap(gray);
% xlabel('Pixels');
% ylabel('Pixels');
xlabel('[m]'); ylabel('[m]');

run_time(toc)

default = 'No'; button = questdlg('Save the Figure?','Figure
Save','Yes','No',default);

%%%%%%%%%%%%%%%%%%%%  To Save the figures Developed  %%%%%%%%%%%%%%%%%%%%
if strcmp(button,'Yes')
    load lastname
```

```
    disp(['last file name used ->', filename]);
    filename   = input('File Name -> ','s');
    %filename2 = input('File Name 2 -> ','s');
    path1      = 'I:\thesis\My_Thesis2\Chapter4\figures\';
    save('lastname','filename');
    print('-depsc2','-tiff','-f1',[path1 filename]); %saves figures
    print('-depsc2','-tiff','-f2',[path1 filename2]);
end


%%%%%%%%%%%%%%%%%%%  To Save the Phase Screen Developed  %%%%%%%%%%%%%%%%
if auto == 0 || auto == 1
    v_save = input('Do you want to save a variable? 0 No/ 1 Yes ->');clc;
    if v_save
    [f_name,v_name] = set_save(auto);
    save(f_name,v_name)
    end
elseif auto == 2
    disp('saving slides')
    [f_name,v_name] = set_save(auto);
     save(f_name,'h_PhScrn')
end
```

A.2 Linear and Quadrant Method for Beam Steering

```
function [q_PhScrn]=q_steer(x_angle,y_angle,num_spots)
%(q_PhScrn)=beam_steer(x_angle,y_angle,varargin)
%function create the Linear and Quadrant method phase screens
%will steer one beam or multiple beams to a specified angle or through
%a specified pattern
```

```
%returns linear phase in units of  waves

N_slm  = 512;\\
ds     = 7.68e-3/N_slm;\\
lambda = 632.8e-9;\\
k      = 2*pi/lambda;\\

%%%%%%%%%%%%%%%%%  Linear Phase screen Development  %%%%%%%%%%%%%%%%%%%%%
n_spot = 512/(num_spots/2); %this may become func call in the future
tilt   = zeros(n_spot,n_spot,num_spots);

%loop to create Linear and Quadrant method phase screens
for ii = 1:size(x_angle,2)
    if num_spots == 1
        tilt   = linear_tilt(N_slm,ds,x_angle(ii),-y_angle(ii));
        phase  = tilt(:,:,1);
    else
        %loop to create individual spot phase screen
        for jj = 1:num_spots
            tilt(:,:,jj)...
               = linear_tilt(n_spot,ds,x_angle(jj,ii),-y_angle(jj,ii));
        end
        %build final phase screen in spatial units
        phase  = [tilt(:,:,1) tilt(:,:,2)
                  tilt(:,:,3) tilt(:,:,4)];
    end

    u = exp(j*k*phase);
```

```
    if size(x_angle,2) == 1
        q_PhScrn = fliplr(angle(u)/(2*pi));
    else
        q_PhScrn(:,:,ii)=fliplr(angle(u)/(2*pi));
    end
end
```

A.3 Holographic Algorithm

```
function [h_PhScrn] = h_steer(U_in,max_iter,auto)
%[PhScrn]=h_steer(U_in,max_iter,auto)
%This function perfroms the Gerchberg_saxton phase algorithm to develop
%the holographic phase maps
%returns holographic phase in waves

if ~auto
    SEE   = input('Want to see the image being built? 0 no/1 yes ->');clc;
else
    SEE   = 0;
end

field_amp = .0025/4; %amplitude of the incoming field
L = field_amp.*ones(size(U_in,1),size(U_in,2));\\
h_PhScrn = zeros(size(U_in,1),size(U_in,2),size(U_in,3));\\
```

```
%%%%%%%%%%%%%%%%%%%%%%%%%%%%%%%%%%%%%%%%%%%%%%%%%%%%%%%%%%%%%%%%%%%%%%%%%%%%
%                    START THE HOLOGRAPHIC PHASE ALGORITHM                    %
%%%%%%%%%%%%%%%%%%%%%%%%%%%%%%%%%%%%%%%%%%%%%%%%%%%%%%%%%%%%%%%%%%%%%%%%%%%%
for nn = 1:size(U_in,3)

     U_desired = abs(U_in(:,:,nn)); %this is the desired image

    %The first step is to start with a uniform random phase pattern
    u_pupil_plane = L.*exp(j*rand(size(U_in,1),size(U_in,2)));

    %propagate field with radnom phase to the far field
    U_image_plane = ft2(u_sim);

    kk   = 0;
    flag = 0;

    %%%%%%%%%%%%%%%%%%% HERE IS WHERE ITERATIVE PART BEGINS %%%%%%%%%%%%%%%
    while kk < max_iter
        %replace phase with desired phase
        U_image_plane = U_desired.*exp(j*angle(U_image_plane));

        %prop back to SLM and replace with laser amp
        U_pupil_plane = L.*exp(j*angle(ift2(U_image_plane)));

        %prop to far field
        U_image_plane = ft2(U_pupil_plane);

        if SEE
            figure(1)
```

```
            imagesc(abs(U_image_plane).^2)
            colormap('gray')
            pause(.1);
           % make_movie(60);
        end

        kk = kk+1;
    end

    if size(U_in,3)== 1  %used when multpile phases screens are produced
        h_PhScrn = fliplr(angle(U__pupil_plane)/(2*pi));
    else
        %for single phase screens
        h_PhScrn(:,:,nn) = fliplr(angle(U__pupil_plane)/(2*pi));
    end
end
```

A.4 Propagate Phase Screen to Far Field

```
function [U_out]=PhScrn_view(PhScrn,auto,varargin)
% [U_out] = PhScrn_view(PhScrn,x,y,auto,varargin)
% takes phase screens and displays what is seen in the image plane
% the power to which "abs(U).^view_pow" is displayed is variable but the
% default is 2
% Also an aperture can be placed in front of the phase screen
% ex. PhScrn_view(PhScrn,x,y,view_pow,'circ', size of ap_diam in meters) or
% ex. PhScrn_view(PhScrn,x,y,view_pow,'rect', size rect in x & y in meters)
% An avi file can be made of the images produced in this m-file.
% The program will prompt the user to see if they would like to make movie
```

```
if nargin > 2
    view_pow = varargin{1};
else
    view_pow = 2;
end

if nargin > 3
    x = varargin{2};\\
    y = varargin{3};\\
    if strcmp('circ',varargin{4})
        sz_ap   = varargin{5};
        ap      = circ(x,y,sz_ap);
    elseif strcmp('rect',varargin{4})
        sz_ap_x = varargin{5};
        if isempty(varargin{6})
            sz_ap_y = varargin{5};
        else
            sz_ap_y = varargin{6};
        end
        ap = rect(x,sz_ap_x).*rect(y,sz_ap_y);
    end
else
    ap = 1;
end

if size(PhScrn,3)== 1  %if only one phase screen is passed in
     u = exp(j*2*pi*fliplr(PhScrn)) .* ap;
     U_out = ft2(u);
```

```
      if ~auto

         figure(1)
         imagesc(abs(U_out).^view_pow)
         %imagesc(PhScrn)
         set(gca,'fontsize',20)
         %axis off
         xlabel('Pixels')
         ylabel('Pixels')
         colormap('gray')
         img_prep(U_out);
      end
else
    first = 1;
    for ii = 1:size(PhScrn,3) %if multiple phase screen are passed in
        u  = exp(j*2*pi*fliplr(PhScrn(:,:,ii)));
        U  = ft2(u);
        U_out(:,:,ii) = U;

         if ~auto
             figure(1)
             imagesc(abs(U).^view_pow)
%             axis off;
             colormap('gray');
%             pause(.5);
%             if first
%             button=questdlg('Make Movie?','Movie Check','Yes','No','No');
%             first = 0;
%             if strcmp(button,'No'), disp('No Movie Made'); end
```

```
%              end
%              if strcmp(button,'Yes')
%                  make_movie(size(PhScrn,3))
%              end
           end
%          img_prep(U_out);
    end %end for
end %end if
```

A.5 Holographic Tracking Method

```
%This m_file was used for applying phase screens on the SLM. However in
%the form showed below, the Holographic Tracking method is shown.
%It loads a saved sequence of Quadrant method phase screens into MATLAB
%then loads them into the SLMs memory.  When the SLM Quadrant method phase
%screen is loaded and applied on the SLM then an function is called to load
%the get an image produced by the camera.  The holographic algorithm is
%then uses the camera image to iterate upon.  When the holographic phase
%screen is produced it is applied on the second SLM.  This process
%continues for how ever many Quadrant method phase screens were loaded.
%When an image is to be taken the holographic SLM is commanded to all zeros
%so that an image can be taken of the Quadrant method spots.  If the
%holographic method spots were still on the Quadrant method spots then when
%the image was taken between the holographic spots would be in the image
%and sebsequently the holographic algortihm would produce those spots as
%well.  To avoid this the holographic SLM is commanded to zeros which puts
%the spots in the center of the image.  This center spot is then covered up
%in post image processing before the image is given to the holographic
%algorithm as the desired image in to build the necessary phase screen.
```

```
%%%%%%%%%%%%%%%%%%%%%%%%  Intialize the SLM  %%%%%%%%%%%%%%%%%%%%%%%%%%%%%%%
slm_ini = 1;\\
if slm_ini  == 0;
    slm_man = slm_manager();
    slm_man = initialize(slm_man);
    slm6035 = slm(1);
    slm6035 = choose_SN(slm6035, '6035');
    [flag1, slm_man, slm6035] = enable_slm(slm_man, slm6035);

    slm7084 = slm(2);
    slm7084 = choose_SN(slm7084, '7084');
    [flag1, slm_man, slm7084] = enable_slm(slm_man, slm7084);
end

%%%%Constants
clc;
lambda      = 632.8e-9;           %wave length of HeNe laser
k           = 2*pi/lambda;        %wave number
N_slm       = 512;                %number of pixels in SLM device
sz_SLM      = 7.68e-3;            %physical size of the slm
ds          = sz_SLM/N_slm;       %differential spatial distance

%%%%%%%%%%%%%%%%%%%%%%%%  Load Saved Phase Screens  %%%%%%%%%%%%%%%%%%%%%%%%
q_PhScrn    = load_screen;
%h_PhScrn   = load_screen;
%Z          = zeros(N_PhScrn);
%q_PhScrn   = fliplr(q_PhScrn(:,:,1));
%h_PhScrn   = fliplr(h_PhScrn);
```

```
%%%%%%%%%%%%%%%%  Load and Apply Phase Screen onto SLM  %%%%%%%%%%%%%%%%
load_phase(slm6035,q_SLM,1:size(q_PhScrn,3));
% load_phase(slm6035,Z,1);  %for applying zero phase

apply_phase(slm6035,1); disp('Quad Screen: 1');
% load_phase(slm7084,h_PhScrn,1);
load_phase(slm7084,Z,1); apply_phase(slm7084,1); disp('Zeros on
Holographic SLM')

%%%%%%% Get Image of of the Camera
%this function does some post processing on the image after it is loaded
%into {\mat}
cam_im = im_detect;

%%This calls the correcting Algorithhm
U_d = im_desired(cam_im);

%Send desired image to the holographic algorithm
h_PhScrn = h_steer(U_d,1,1);

%Load the phase screen developed on the holographic PhScrn
load_phase(slm7084,h_PhScrn,2); apply_phase(slm7084,2);

%%%% Enter the Tracking Loop
for idx = 2:size(q_PhScrn,3)
    %Apply the Quad phase
    apply_phase(slm6035,idx);
```

```
    disp(['Quad Screen: ' num2str(idx)]);

    %%Prep to take image
    pause(2)
    apply_phase(slm7084,1);
    cam_im = im_detect; %get image off camera
    apply_phase(slm7084,idx); %puts old holo image back on

    U_d = im_desired(cam_im);
    disp('Developing Holographic Phase')

    %tic;
    h_PhScrn = h_steer(U_d,1,1);
    rec_h_PhScrn(:,:,idx)=h_PhScrn;
    %run_time(toc)
    disp(['Holo Screen' num2str(idx)]);
    load_phase(slm7084,h_SLM,idx+1);
    apply_phase(slm7084,idx+1);
    pause(2)
end

disp('Ready to show it all happen at once');%clc;
pause

%%Due to hardware limitations the traking algorithm can be hard to follow
%when viewing on the camera, so once all of the holographic the phase
%have been developed and loaded into the SLM's memory the whole sequence
%can be replayed. This gives a pseudo representaiotn of what the whole
%process would look like if the right equipment was used.
```

```
while 1
    apply_phase(slm7084,1);
    for idx = 1:size(q_SLM,3)
        apply_phase(slm6035,idx);
        apply_phase(slm7084,idx+1);
        pause(.5)
    end
    pause(2)
end
```

```
%%%%%%%%%%%%%%%%%%%%%%  Shut down sequence for SLM  %%%%%%%%%%%%%%%%%%%%%%
[flag2, slm_man, slm6035] = disable_slm(slm_man, slm6035); [flag2,
slm_man, slm7084] = disable_slm(slm_man, slm7084); slm_man =
finalize(slm_man);
```

A.6 Correcting Algorithm

```
function gauss = im_desired(img)
%gauss = desired_im
%this funtion takes in an image and determines the location of the spots in
%each of the four quadrants and then builds an image with gaussian spots in
%the location of each respective quadrants maximum

%%%%%%%%%%%%%%%%%%%%%%%%  Split Image into Quadrants  %%%%%%%%%%%%%%%%%%%%
q1 = img(1:256,1:256);\\
q2 = img(1:256,257:512);\\
q3 = img(257:512,1:256); \\
q4 = img(257:512,257:512);\\
```

```
%locate the max in each quadrant
[y1 x1] = find(q1 == max(max(q1)),1); \\
[y2 x2] = find(q2 == max(max(q2)),1);\\
[y3 x3] = find(q3 == max(max(q3)),1); \\
[y4 x4] = find(q4 == max(max(q4)),1);

x_loc   = [257-x1    -x2 257-x3 -x4];\\
y_loc   = [257-y1 257-y2 -y3 -y4];\\
%%%pixel location conversion from det. pixels to im. plane pixels
for kk  = 1:length(x_loc)
    %pixel conversion when 250 mm focal length lens is used
    x_loc(kk) = round(x_loc(kk)*7.5e-6 / 20.6e-6);
    y_loc(kk) = round(y_loc(kk)*7.5e-6 / 20.6e-6);

    %pixel conversion when 1m focal length lens is used
    x_loc(kk) = round(x_loc(kk)*7.5e-6 / 82.4e-6);
    y_loc(kk) = round(y_loc(kk)*7.5e-6 / 82.4e-6);
end\\
a = 1;
w = 1;  %desired radial pixel width of the Gaussian spot
[x_g y_g] = meshgrid(-512/2:512/2-1);
%puts Gaussian spot at respective spot locations
for ii = 1:4
    field(:,:,ii) = a*exp(-2*((x_g+x_loc(ii)).^2+(y_g+y_loc(ii)).^2)/w^2);
end
%Combine each Gaussian frame into one desired image to send to the
%Holographic algorithm
gauss = mean(field,3);
```

A.7 Load Image from Camera

```
function img = im_detect;
%img = img_detect;
%this m file is a polling program which constantly looks for an image to be
%added to a specified directory when that happens it will plot and process
%the image.  This processing involves thresholoding the image to reduce the
%background irradiance, and a mask to cover up the center spot produced by
%the holographic SLM while in the tracking loop.

%%%%  Designated folder where the camera deposits the images taken  %%%%%%
d_folder  = 'L:\eng students\SLM_screens\Mawhorter_Screens\Camera_Images\';\\
n_date    = date;\\
n_date    = [n_date(4:6) ' ' n_date(1:2) ' ' n_date(8:11)];
folder    = [d_folder n_date '\']; \\
files     = dir(fullfile(folder,'*.bmp'));\\
sz_old    = size(files,1);\\
img       = zeros(512);

%%%%%%%%%%%%%%%%  Enter Loop to Wait For an Image to be Taken  %%%%%%%%%%
disp('Ready To Capture Image'); while 1
   files  = dir(fullfile(folder,'*.bmp'));
   sz     = size(files,1);
   if sz  > sz_old
     img3 = double(imread([folder 'FRAME_' num2str(sz-1) '.bmp']));
     img2 = mat_fr(img3,100,0);           %performs the thresholding
     img  = img2.*onespad(zeros(32),512); %builds mask to cover center spot

     %figure;imagesc(img);colormap gray;
     %d   = RED(img,'centroid',0);
```

```
     sz_old = sz_old + 1;
     %peak  = max(max(img))
     break;
   end
   pause(.5);
end
```

A.8 Image Preparation for Thesis

```
function img_prep(img)
%function img_prep(img)
%This function gets an image ready to be input into thesis
%It will normalize the image then obtain a reversed image
%If the image is a camera image then thresholding is done on the image so
%that only the spot appears black and the back ground is as close to white
%as can be achieved.

lambda   = 632.8e-9;           %wave length of HeNe laser
k        = 2*pi/lambda;        %wave number
f        = .250;               %m focal length
N_slm    = 512;                %number of pixels in SLM device
N_img    = N_slm*2;            %used when zero padding
sz_SLM   = 7.68e-3;            %physical size of the slm
ds       = sz_SLM/N_slm;       %differential spatial distance
df       = lambda*f/(N_slm*ds);%differential frequency
dc       = 7.5e-6;             %camera pixel size

[x,y]    = meshgrid((-N_slm/2:N_slm/2-1)*ds);
[u,v]    = meshgrid((-N_slm/2:N_slm/2-1)*df);\\
[cu,cv]  = meshgrid((-N_slm/2:N_slm/2-1)*dc);\\
```

```
x_plot   = x(257,:);%used to get physical dimensions on images if needed
u_plot   = u(257,:); \\
cu_plot  = cu(257,:);\\
img2     = abs(img).^2;

Mn       = min(min(img2));\\
Mx       = max(max(img2));\\
IMG_Norm = (img2-Mn)/Mx;\\
img_reversed = 1-IMG_Norm;\\

figure(2) set(gca,'fontsize',20)
% imagesc(u_plot,u_plot,img_reversed)
imagesc(cu_plot,cu_plot,img_reversed) colormap(gray);
% xlabel('Pixels');
% ylabel('Pixels');
xlabel('[m]'); ylabel('[m]');\\
ZoomVec = dc*[-6 170 -75 75]; \\
axis(ZoomVec);
```

A.9 Load Phase Screen

```
function screen = load_screen
%screen = load_screen will load a phase screen that has been developed
%my default directory
d_folder      = ...
'L:\engstudents\SLM_screens\Mawhorter_Screens\Beam_Steering';

    prompt    = {'Screen to load? ','Directory'};
    dlg_title = 'Screen loader';
    num_lines = 1;
    default   = {'',d_folder};
    name      = inputdlg(prompt,dlg_title,num_lines,default);

    scrn_name = char(name{1});
    dir_name  = char(name{2});

    try
        data  = load([dir_name '\' scrn_name]);
    catch
        Errordlg('Please enter correct filepath','Error');
    end

   %get variable from loaded file
    name      = cell2mat(fieldnames(data));
    %there should only be one variable
    statement = ['data.',name];
    screen    = eval(statement);
```

A.10 Save Phase Screen

```
function [f_name,v_name] = set_save(auto) folder = ...
'L:\engstudents\SLM_screens\Mawhorter_Screens\Beam_Steering\';

persistent slide\\
if isempty(slide)
   slide  = 1;
end

if auto == 2
    f_name    = [folder 'Holo_' num2str(slide)];
%   save(f_name,'q_SLM');
%   f_name    = [folder date '_2'];
    save(f_name,'h_SLM');
%   f_name    = [folder date '_slides'];
%   save(f_name,'slides');
%   slide     = slide + 1;\\
else
    prompt    = {'Which variable:','File name:','Directory'};
    dlg_title = 'Variable to Save';
    num_lines = 1;
    default   = {'','',folder};
    name      = inputdlg(prompt,dlg_title,num_lines,default);
    f_name    = [char(name{3}) '\' char(name{2})];
    v_name    = char(name{1});
end
```

Bibliography

1. Bifano T., Bierden P., Cornelissen S., Dimas C., Lee H., Miller M., and Perreault J. "Large-Scale Metal Mems Mirror Arrays with Integrated Electronics," *The International Society for Optical Engineering (SPIE)*, *4755*:467–476 (2002).

2. Boulder Nonlinear Systems, 450 Courtney Way, Unit 107, Layfayette, CO 80026. *User Manual: 512x512 SLM System* (Third Edition), December 2004.

3. Goodman J. W. *Introduction to Fourier Optics* (Third Edition). San Fransico, CA: Roberts and Company, 2005.

4. Gruneisen M. T. and DeSandre L. F. "Programmable diffractive optics for widedynamic-range wavefront control using liquidcrystal spatial light modulators," *The International Society for Optical Engineering (SPIE)*, *4825*:1387–1393 (2002).

5. Gu D.-F., Winker B., Taber D., Cheung J., Lu Y., Kobrin P., and Zhuang Z. "Dual Frequency Liquid Crystal Devices for Infrared Electro-Optical Applications," *The International Society for Optical Engineering (SPIE)*, *4799*:37–47 (2002).

6. Harris S. "Characterization and Application of a Liquid Crystal Beam Steering Device," *The International Society for Optical Engineering (SPIE)*, *4291*:109–119 (2001).

7. Hällstig E., Sjöqvist L., and Lindgren M. "Characterization of depolarizing fringing fields of a liquid crystal spatial light modulator for laser beam steering," *The International Society for Optical Engineering (SPIE)*, *5237*:167–177 (2004).

8. Hect E. *Optics* (Fourth Edition). Englewood, CO: Addison Wesley, 2002.

9. Oliver S. S. "Advanced adaptive optics technology development," *The International Society for Optical Engineering (SPIE)*, *4494*:1–10 (2002).

10. Perry M. J. *Using liquid crystal spatial light modulators for closed loop tracking and beam steering with phase holography*. MS thesis, Graduate School of Engineering, Air Force Institute of Technology (AETC), Wright-Patterson AFB OH, March 2005. AFIT/GEO/ENG/05-02.

11. Stockley J., Serati S., Xun X., and Cohn R. W. "Liquid Crystal Spatial Light Modulator for Multispot Beam Steering," *The International Society for Optical Engineering (SPIE)*, *5160*:208–215 (2004).

12. Welsh B., Roggemann M. C., and Wilson G. L. "Phase retrieval based algorithms for far field beam steering and shaping," *The International Society for Optical Engineering (SPIE)*, *3763*:11–22 (1999).

REPORT DOCUMENTATION PAGE

Form Approved
OMB No. 0704–0188

1. REPORT DATE *(DD–MM–YYYY)*	2. REPORT TYPE	3. DATES COVERED *(From — To)*
23–03–2006	Master's Thesis	Sept 2004 — Mar 2006

4. TITLE AND SUBTITLE

Active Optical Tracking with
Spatial Light Modulators

5a. CONTRACT NUMBER

5b. GRANT NUMBER

5c. PROGRAM ELEMENT NUMBER

6. AUTHOR(S)

Steven Mawhorter, 2d Lt, USAF

5d. PROJECT NUMBER

JON–06–346

5e. TASK NUMBER

5f. WORK UNIT NUMBER

7. PERFORMING ORGANIZATION NAME(S) AND ADDRESS(ES)

Air Force Institute of Technology
Graduate School of Engineering and Management (AFIT/EN)
2950 Hobson Way Bldg 640
WPAFB OH 45433-7765

8. PERFORMING ORGANIZATION REPORT NUMBER

AFIT/GE/ENG/06-40

9. SPONSORING / MONITORING AGENCY NAME(S) AND ADDRESS(ES)

AFMC/AFRL/SNJM
Mike Perry, Capt, USAF
3109 Hobson Way Bldg 622
WPAB, OH 45433-7700
DSN: 785-9614 x 282 COMM:(937) 255-9614 x 282
email: Micheal.Perry@wpafb.af.mil

10. SPONSOR/MONITOR'S ACRONYM(S)

11. SPONSOR/MONITOR'S REPORT NUMBER(S)

12. DISTRIBUTION / AVAILABILITY STATEMENT

Approved for public release; distribution unlimited

13. SUPPLEMENTARY NOTES

14. ABSTRACT

Two spatial light modulators are utilized for beam splitting, steering and tracking. Both linear and holographic phase screens are used in a demonstration of technology to allow real time tracking to communicate in a one-to-several type scenario. One SLM is used to apply a linear phase modulation to steer multiple beams onto a detector. The spots that are produced represent the targets as they move around the field of view of the central communication node. A Gerchberg-Saxton algorithm will subsequently use the detected spots as the desired pointing locations. Using this as input, the Gerchberg-Saxton algorithm yields a phase only map, for multiple spot beam steering which is called the holographic phase. The holographic phase screens are then used on a second SLM to steer beams on the same detector in near real time. As the target spots move about the detector's field of view the holographic spots track them.

15. SUBJECT TERMS

holographic beam steering, Gerchberg-Saxton Phase Retrieval, spatial light modulator, optical tracking, wavefront control

16. SECURITY CLASSIFICATION OF:			17. LIMITATION OF ABSTRACT	18. NUMBER OF PAGES	19a. NAME OF RESPONSIBLE PERSON
a. REPORT	b. ABSTRACT	c. THIS PAGE			Lt Col Goda
U	U	U	UU	95	19b. TELEPHONE NUMBER *(include area code)* (937) 255-3636 x 4614